Earth's Future

RESEARCH ARTICLE
10.1029/2021EF002572

Delimiting China's Urban Growth Boundaries Under Localized Shared Socioeconomic Pathways and Various Urban Expansion Modes

Miao Huang[1,2], Zichen Wang[1,2], Xinhao Pan[1,2], Binghua Gong[1,2], Mengzhao Tu[3], and Zhifeng Liu[1,2]

[1]State Key Laboratory of Earth Surface Processes and Resource Ecology (ESPRE), Beijing Normal University, Beijing, China, [2]Faculty of Geographical Science, School of Natural Resources, Beijing Normal University, Beijing, China, [3]Consulting & Research Center, Ministry of Natural Resources, Beijing, China

Key Points:

- The extent of China's urban growth boundary was projected to be 34.14–58.25% higher than the urban area in 2020
- China's urban land demand in 2100 would be lower than the extent of UGBs, implying China will face remarkable urban shrinkage pressure
- China should take effective measures to address the urban shrinkage pressure and reduce the negative impacts from urban expansion

Supporting Information:

Supporting Information may be found in the online version of this article.

Correspondence to:

Z. Liu,
zhifeng.liu@bnu.edu.cn

Citation:

Huang, M., Wang, Z., Pan, X., Gong, B., Tu, M., & Liu, Z. (2022). Delimiting China's urban growth boundaries under localized shared socioeconomic pathways and various urban expansion modes. *Earth's Future*, *10*, e2021EF002572. https://doi.org/10.1029/2021EF002572

Received 24 NOV 2021
Accepted 5 JUN 2022

Author Contributions:

Conceptualization: Zhifeng Liu
Data curation: Miao Huang, Zichen Wang, Xinhao Pan
Formal analysis: Miao Huang
Funding acquisition: Zhifeng Liu
Methodology: Zhifeng Liu
Project Administration: Zhifeng Liu
Resources: Zhifeng Liu
Software: Miao Huang, Zichen Wang, Xinhao Pan
Supervision: Zhifeng Liu

Abstract Delimiting the urban growth boundary (UGB) is important for limiting urban sprawl and improving urban sustainability. However, the future UGB delimitation for the entire China is still lacking. Here, we delimited China's UGBs before 2100 under localized shared socioeconomic pathways and 11 urban expansion modes (i.e., spontaneous growth, organic growth, and nine modes integrating both) and evaluated the urban shrinkage pressure and the effects on other land use/cover types and ecosystem services. The results revealed that China's urban land demand was projected to increase first and then decrease under five scenarios before 2100. The extent of UGBs was projected to be 121,199–142,982 km^2, 34.14–58.25% higher than the urban area in 2020. As a result of urban population decline, China's urban land demand in 2100 was projected to be 20.83–53.41% lower than the extent of UGBs, implying that China, especially the three provinces of Heilongjiang, Jilin, and Liaoning, will face remarkable urban shrinkage pressure. Future urban expansion in China will mainly occupy cropland, and lead to a simultaneous decline in habitat quality, food production and carbon sequestration. Spontaneous growth will cause greater losses of ecosystem services than organic growth at the national scale, while in some provinces, such a difference will be reversed. To address the urban shrinkage pressure, China needs to control urban area and optimize urban spatial patterns based on UGBs. In addition, the place-based optimal urban expansion mode is also required to reduce the negative impacts of future urban expansion on ecosystem services and promote sustainable development.

Plain Language Summary Urban expansion has caused a series of ecological and social problems. Therefore, setting urban growth boundaries around cities to limit urban sprawl within such boundaries and reduce its negative impacts has been a critical way for sustainable development. This study delimited China's urban growth boundaries before 2100 under five scenarios of localized shared socioeconomic pathways and 11 urban expansion modes (i.e., spontaneous growth, organic growth, and nine modes integrating both) and evaluated the potential effects of future urban expansion on urban shrinkage pressure, other land use/cover types and ecosystem services. The results showed that China's urban land demand was projected to show an increasing trend followed by a decrease under five scenarios from 2021 to 2100, leading to a nationwide urban shrinkage pressure, and the effects of future urban expansion on ecosystem services varied with urban expansion modes. This study suggests that China, especially the three provinces of Heilongjiang, Jilin, and Liaoning, should take measures to optimize urban spatial patterns and address urban shrinkage pressure, and each province needs to take the place-based optimal urban expansion mode based on the environmental, social, and economic characteristics to improve urban sustainability.

1. Introduction

Urban expansion has caused a series of problems, such as losses of natural habitats, reduction of cropland, environmental pollution, and so on (Grimm et al., 2008; Seto et al., 2012; Wu, 2014; Ye et al., 2020). To limit urban sprawl and reduce the negative impacts of urban expansion, the United States has taken the lead in delimiting urban growth boundaries (UGBs), that is, setting boundaries around cities and limiting urban expansion within such boundaries (Daniels, 2001). This approach can effectively protect the cropland and natural habitat around cities (Wei & Ye, 2014), alleviating the contradiction between urban development and the conservation of resources and environment to realize sustainable development (Jiang, Chen, et al., 2016; Long et al., 2013; Tayyebi et al., 2011). In China, where the urban land area (ULA) is increasing rapidly, delimiting UGBs has

Visualization: Miao Huang
Writing – original draft: Miao Huang
Writing – review & editing: Binghua Gong, Mengzhao Tu, Zhifeng Liu

been explicitly included in the *Measures for Formulating City Planning* published by the Ministry of Housing and Urban-Rural Development in 2005 (Ministry of Housing and Urban-Rural Development of PRC, 2005) and the *Guiding Opinions on the Overall Planning for Land Use at the City, County, and Township Levels* in 2009 (Ministry of Land and Resources of PRC, 2009). The delimitation of the UGB has been a critical way to improve urban sustainability in China (Jiang, Cheng, et al., 2016; Long & Mao, 2010).

As an effective urban planning and management method implemented worldwide (Bengston & Yeo-Chang, 2006; Gennaio et al., 2009; Han et al., 2009; Jun 2004; Mubarak, 2004), the delimitation of UGBs has been studied for a long time. Currently, most of the UGBs in practice are mainly based on local policies, development needs and experts' experiences (Chettry & Surawar, 2021; Yang, Zhang, et al., 2019). For example, experience-based UGBs were first qualitatively established and then delineated according to different development needs in Portland, Oregon, USA (The Nature of 2040, 2000). However, this planning method usually lacks sufficient scientific evidences and quantitative analyses, which is considered to be possibly not well adapted for the complex urban growth in the future (Long et al., 2013). In addition, more studies were conducted on the quantitative UGB delineation based on the land use suitability evaluation (Bhatta, 2009; Cerreta & De Toro, 2012; Ma et al., 2017). For example, Wang et al. (2012) delineated the rigid UGBs and elastic UGBs based on the land ecological suitability. Ye et al. (2015) provided references for future UGB delineation by measuring ecological resistance to urban expansion. By combing the ecoenvironmental sensitivity and urban residential activity, Jia et al. (2019) evaluated the urban expansion potential and delimitated future UGBs based on the predicted urban expansion scale. However, given numerous natural and socioeconomic factors which influence urban growth in complex ways at different spatial-temporal scales, these simple UGB delineation methods based on the suitability or restriction evaluation have limitations (Liang et al., 2018) and cannot effectively be used in future urban planning and development (Ma et al., 2017).

Instead, with the development of remote sensing and geographic information system, the methods of simulating urban dynamics based on urban models and delineating UGB based on the simulation results were widely used and had become a common way to quantitatively delineate UGB (Wang et al., 2014). The main idea of these approaches is to estimate the urban land demand (ULD) according to environmental suitability and carrying capacity first and then simulate the potential urban spatial patterns by using urban expansion models to determine the maximum urban growth range (Tan et al., 2020). For example, Long et al. (2009) obtained the ULA through the urban master plan and developed UGBs based on a constrained CA model. Sakieh et al. (2015) determined the ULD based on the historical urban growth trend, simulated the spatially explicit probability of urban expansion by using the slope, land use, exclusion, urban, transportation, hillshade (SLEUTH) model, and used a threshold to define UGBs. Liang et al. (2018) estimated the ULD based on the system dynamics model and then performed morphological dilation and erosion on the simulation results of the Future Land Use Simulation (FLUS) model to delineate the UGBs. Gantumur et al. (2020) calculated the ULD by using the analytic hierarchy process method and realized spatial simulation and UGB delimitation through an artificial neural network-cellular automata (ANN-CA) model. Tariq and Shu (2020) estimated the future ULD by using Markov chains and simulated the spatial pattern of urban land based on the CA model. In addition, CA models optimized with logistic regression (Liu, Zhang, et al., 2017), ant colony optimization (Ma et al., 2017), particle swarm optimization (Feng et al., 2018), genetic algorithm (Yang, Gong, et al., 2019), or coupled with models such as soil conservation services (Xu et al., 2013), comprehensive ecological security (Cong et al., 2018), and dual-environmental evaluation (Zhang et al., 2020) have also been widely used in delimiting UGBs.

Existing studies have built a good foundation for China's UGB delimitation, yet there are still some inadequacies. First, the UGB delimitation of China is concentrated at the scale of city or urban agglomeration (Wang et al., 2014). Relevant research at the national scale only includes the delimitation results of historical urban boundaries (Li et al., 2020), lacking research on the future UGB delineation of China. For example, Long et al. (2009) delimited UGBs in Beijing. Wu et al. (2017) identified UGBs in the Yangtze River Delta urban agglomeration. Liang et al. (2018) delineated UGBs in the Pearl River Delta region. Second, related research needs to be improved in both ULD estimation and urban spatial pattern simulation. In terms of ULD estimation, owing to a lack of a unified framework for scenario setting, the simulated ULDs are incomparable under different scenarios and scales in previous studies (Feng et al., 2019; Guo & Huang, 2018; Zhang et al., 2011). In terms of urban spatial pattern simulation, existing urban models used in China's future UGB delineation cannot effectively

simulate urban expansion under diverse urban expansion modes, making it difficult to fully demonstrate the potential urban spatial patterns in the future (Chen et al., 2019; Meentemeyer et al., 2013).

Shared socioeconomic pathways (SSPs) provide a reliable framework for China's future ULD estimation. SSPs, a set of socioeconomic pathways with a basic analysis unit of country, were released by the Intergovernmental Panel on Climate Change (IPCC). By considering population, economic, policy, technology, environment, resource, and other factors and combining mitigation and adaptation to climate change challenges, SSPs provide a unified framework for global urban expansion simulation and have been widely used in future global urban development and economic growth forecasts (Jiang & O Neill, 2017; O'Neill et al., 2014, 2017). However, the original SSPs still have some inadequacies in future population estimations of China, limiting their ability to predict China's future urban development. The reasons are as follows: (a) the outdated population in 2000 is used as initial input data in the population projection model, (b) the parameters of the population projection model have not been modified according to national population conditions and policies, such as the two-child policy, and (c) with a basic simulated unit of country, provincial development differences have not been considered (Jiang et al., 2017, 2018). In response to those inadequacies, Chen, Guo, et al. (2020) localized the original SSPs by considering family planning and household registration policies in China and reestimated the provincial population and urban share under SSPs from 2010 to 2100 by considering the impacts of development policies adjustments such as "two-child policy," "compulsory education policy," and population ceiling policies in megacities. The localized SSPs provide a more reliable scenario framework and basic data for future ULD estimation in China.

Models such as FLUS (Liu, Liang, et al., 2017), Country-Level Urban Buildup Scenario-Spatially Explicit, Long-term, Empirical City development (CLUBS-SELECT) (Gao & O'Neill, 2020), SLEUTH (Zhou et al., 2019), UrbanMOD (Seto et al., 2012), CLUMondo (van Asselen & Verburg, 2013), and Land Use Scenarios Dynamics Model-urban (LUSD-urban) (He et al., 2016, 2021; He, Li, et al., 2017) are commonly used in urban expansion simulations. Researchers have simulated global and Chinese urban spatial patterns by using the urban expansion models above, providing the spatial distribution of future urban land for delimiting UGBs in China. However, urban expansion was always presented by the state transition of individual pixels during each simulation iteration in these traditional CA models (Li & Gong, 2016), which has difficulty reflecting the actual urban expansion in patches and has limited ability to effectively simulate urban growth under diverse urban expansion modes (Chen et al., 2014; Hu et al., 2016). The patch-based urban model with an additional module to simulate changes in urban patches is another form of CA model in urban growth modeling (Li et al., 2017), which has been continuously improved and widely used (Chen, 2022; Dorning et al., 2015; Liang et al., 2021; Soares-Filho et al., 2002; Wang & Marceau, 2013). In addition to improving the accuracy of urban expansion simulations, these urban models with a basic unit of patch composed of several neighboring cells can effectively simulate different urban expansion modes (Chen et al., 2019; Liu et al., 2021; Yang, Gong, et al., 2019).

This study aimed to delimit China's UGBs before 2100 under different scenarios and diverse urban expansion modes. First, the ULD of China from 2021 to 2100 was estimated based on the localized SSPs. Next, the patch-based LUSD-urban model was developed to simulate China's urban spatial pattern from 2021 to 2100 under 11 urban expansion modes (i.e., spontaneous growth, organic growth, and nine modes integrating both) with the province as simulation unit and a spatial resolution of 1 km. Then, China's UGBs were delineated based on the simulation results. Based on UGBs, the pressure of urban shrinkage was analyzed and the potential impacts of urban expansion on habitat quality, food production, and carbon sequestration were evaluated, providing scientific evidence for exploring the optimal path of China's future urban development.

2. Data and Methods

2.1. Data

Urban land data, land use/land cover data, digital elevation model (DEM) data, net primary productivity (NPP) data, GIS auxiliary data, and population data were used in this study (Table 1). The urban land data for 2000–2020 originated from He et al. (2019) at a 1-km spatial resolution, with an overall accuracy of 90.9%. In this data set, urban land is defined as urban built-up area, where the human-constructed elements cover more than 50% of a pixel, excluding rural residential area (Huang et al., 2020; Liu et al., 2014). The land use/land cover data for 2015 were obtained from the Data Center for Resources and Environmental Sciences of the Chinese Academy of

Table 1
Data Description

Data category	Data/Category name	Year	Spatial resolution/overall accuracy
Urban land data	Urban (1) and nonurban (0)	2000–2020	1 km
			90.9%
Land use/land cover data	Cropland, forest, grassland, wetland, bare land, urban land, rural residential area and other construction land, and other land	2015	1 km
			>90%
Digital elevation model data	–	–	1 km
Net primary productivity data	–	2006–2015	1 km
GIS auxiliary data	Administrative boundaries, city centers, roads, and rivers	–	–
	Nature reserves	–	–
Population data	Urban population census data	2005–2015	–
	Population and urban share data under the localized SSPs	2020–2100	–

Sciences (RESDC) (http://www.resdc.cn) featuring a 1-km spatial resolution. This data set was generated from visual interpretation with TM/ETM remote sensing images as the main data source. The overall accuracy of land use/land cover data is 93.00% (Ning et al., 2018). The DEM data originated from the Geospatial Data Cloud Platform of the Computer Network Information Center of the Chinese Academy of Sciences (http://www.gscloud.cn), with a spatial resolution of 1 km. The NPP data for 2006–2015 were acquired from He, Liu, et al. (2017) with a spatial resolution of 1 km. This data set was calculated by using the Carnegie-Ames-Stanford approach (CASA) model based on land use/land cover data, normalized difference vegetation index (NDVI) data, and meteorological data. The GIS auxiliary data include administrative boundaries, city centers, roads and rivers, gathering from the National Geomatics Center of China (http://www.ngcc.cn), and the nature reserves data from RESDC (http://www.resdc.cn). The population data include the provincial urban population census data of China during 2005–2015 from the National Bureau of Statistics (https://data.stats.gov.cn/) and the provincial population and urban share data of China under localized SSPs during 2020–2100 from Chen, Guo, et al. (2020). To ensure data consistency, the coordinate system of raster and vector data was unified to Albers projection, and the spatial resolution of raster data was unified to 1 km.

2.2. Delimitation of UGB

As shown in Figure 1, provincial linear regression models to estimate urban land area were developed based on historical data, and future urban land area in each province was estimated based on the future urban population obtained by localized SSPs. Then, the patch-based LUSD-urban model was developed to simulate urban expansion under diverse modes. Finally, a morphological method was applied to the simulation results to delineate China's UGBs.

2.2.1. Estimation of Urban Land Demand

Referring to He et al. (2021), a linear regression model was used to estimate provincial ULD under five SSPs. According to the *National New Urbanization Planning (2014–2020)* (The State Council of PRC, 2014), considering that China's urban growth was population growth oriented, the urban population was used as an independent variable to estimate the future ULD of China. Specifically, we first developed linear regressions for the historical urban population and ULA in each province using data from 2005 to 2015. Then, we modified the equations to ensure that the regression results based on the urban population in 2020 from localized SSPs in 2020 were consistent with the actual ULA of 2020. The modified equation can be expressed as:

$$A_{i,s}^{t} = \beta_{0_i} + \beta_{1_i} \times UP_{i,s}^{t} + \varepsilon_{i,s} \quad (1)$$

where $A_{i,s}^{t}$ refers to the ULD of province i in year t under scenario s. $UP_{i,s}^{t}$ refers to the urban population of province i in year t under scenario s. β_0 and β_1 refer to the fitting parameters. $\varepsilon_{i,s}$ refers to the modified parameter, which can be expressed as $\varepsilon_{i,s} = A_i^{2020} - \beta_{0_i} - \beta_{1_i} \times UP_{i,s}^{2020}$. The R^2 of all regression equations are greater than

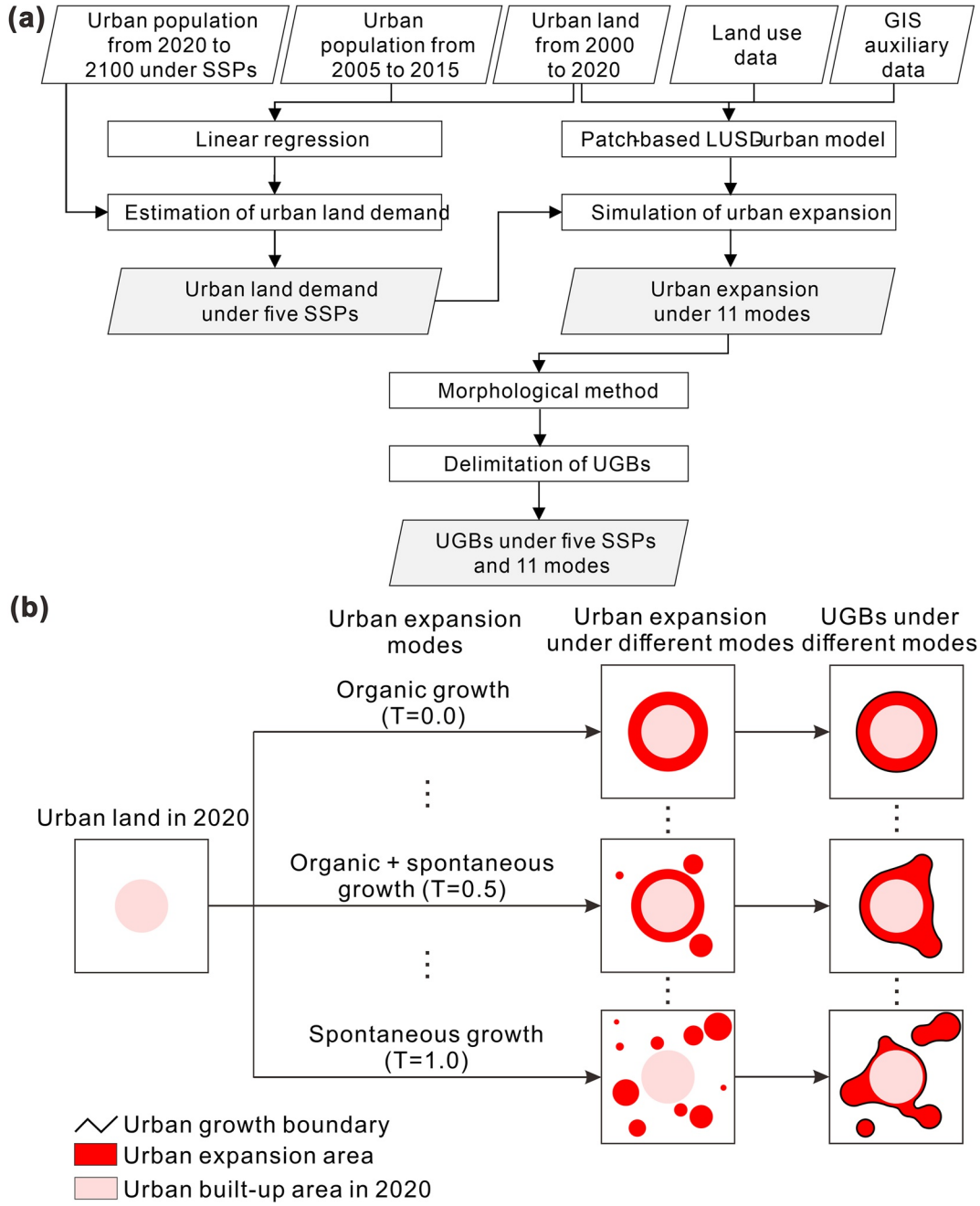

Figure 1. Flowchart (a) and schematic diagram of urban growth boundary delimitation under different urban expansion modes (b). *Note*. T refers to the urban expansion mode index, defined in Section 2.2.2.

0.85 at a 95% significance level. After the establishment of regression equations, we estimated future ULD under five SSPs in each province by using the urban population data provided by localized SSPs.

2.2.2. Spatial Estimation of Urban Expansion

A patch-based LUSD-urban model was developed to simulate future urban expansion in each province. This model adopts the following assumptions: (a) urban areas are projected to expand in patches, and the urban expansion modes of urban patches include organic growth and spontaneous growth (Chen et al., 2014), (b) the transition

from nonurban land to urban land is irreversible, and urban land will not be converted to nonurban land, and (c) the spatial driving factors remain constant during the simulation process.

To simulate urban expansion, the LUSD-urban model calculates the development probability of nonurban pixels converted to urban pixels by integrating suitability factors, inheritance factors, constrained factors and neighborhood effects (He et al., 2006, 2008). The development probability can be expressed as:

$$ {}^{t}P_{K,x,y} = \left(\sum_{j=1}^{m-2} \left(W_j \times {}^{t}S_{j,x,y} \right) + W_{m-1} \times {}^{t}N_{x,y} - W_m \times {}^{t}I_{K,x,y} \right) \times \prod_{r=1}^{R} {}^{t}EC_{r,x,y} \quad (2) $$

where ${}^{t}P_{K,x,y}$ refers to the converted probability from land use type K to urban land in pixel (x,y) and year t. ${}^{t}S_{j,x,y}$ refers to the normalized score of suitability factor j (1, 2, …, $m-2$) ranging from 0 to 100. $m-2$ refers to the number of suitability factors. W_j refers to the weight of suitability factor j. ${}^{t}N_{x,y}$ and W_{m-1} refer to the neighborhood effect in pixel (x,y) and year t and its weight, respectively. ${}^{t}N_{x,y}$ can be expressed as follows:

$$ {}^{t}N_{x,y} = Z \times \sum_{c} (W_c \times {}^{t}G_c) = Z \times \sum_{c} \frac{{}^{t}G_c}{C^Q} \quad (3) $$

where W_c refers to the weight of the influence of urban pixel in the neighborhood at distance C on the conversion of nonurban pixel (x,y) into urban pixel, which can be expressed as a reciprocal of the Q power function with $Q = 1, 2, 3, \ldots$ In this study, Q is defined as 1. ${}^{t}G_c$ is a binary variable equal to in urban pixels and 0 in nonurban pixels at distance C. Z is a scalar used to normalize ${}^{t}N_{x,y}$ between 0 and 100. The window size for the neighborhood effect calculation is defined as 5. ${}^{t}I_{K,x,y}$ refers to the inheritance of land use type K in pixel (x,y) and year t, and W_m refers to its weight. ${}^{t}I_{K,x,y}$ can be defined as a constant value ranging from 0 to 100. The larger the value of ${}^{t}I_{K,x,y}$ is, the greater the inertia of holding the original land use type. ${}^{t}EC_{r,x,y}$ refers to the constrained factors, including high-quality cropland and nature reserves, and R represents the number of constrained factors. Referring to the *Regulation on the Protection of Basic Farmlands* (The State Council of PRC, 2011), high-quality cropland is defined as cropland with NPP ranking in the top 80% in each province.

Based on the LUSD-urban model, urban expansion was simulated in patches with reference to Chen et al. (2014). The size of urban growth patches was calculated according to the power law between the size and quantity of urban growth patches. The equation can be expressed as:

$$ A_l = a_0 (r_{area})^{a_1} \quad (4) $$

where A_l refers to the size of patch l. a_0 and a_1 are the fitting parameters, which can be determined according to the distribution characteristics of the urban patch area in the historical urban expansion. The larger a_1, the more uneven size of urban growth patches (Fragkias & Seto, 2009). r_{area}, a random value of (0,1], represents the probability of selecting a specific patch size from the actual size distribution of urban growth patches.

After determining the area of the new urban growth patch, the urban expansion mode of the new urban growth patch needs to be established to determine its spatial location. Referring to Chen et al. (2014), we defined the urban expansion mode index T as 0.0, 0.1, …, 0.9, 1.0 to indicate 11 urban expansion modes (i.e., spontaneous growth, organic growth, and nine modes integrating both). A random value R_{type}, in the range of [0,1), was used to obtain the urban expansion mode of the urban growth patch. If R_{type} is smaller than the threshold T, the new patch will grow in spontaneous growth; otherwise, it will grow in organic growth. When $T = 0.0$, R_{type} of all new patches is larger than or equal to T, indicating that all urban growth patches will grow in organic growth. When $T = 1.0$, R_{type} of all new patches is smaller than T, indicating that all urban growth patches will grow in spontaneous growth. When T is between 0.0 and 1.0, the new patches will consider both organic and spontaneous growth (Figure 1b). The location of urban growth patches varies with urban expansion modes. For organic growth, the pixel with the highest development probability (Equation 2) was taken as the seed to grow and form a patch. For spontaneous growth, development potential ${}^{t}PO_{K,x,y}$ (Equation 5) was substituted without considering neighborhood effects for development probability (Equation 2) and take the pixel with the highest development potential as a seed. ${}^{t}PO_{K,x,y}$ can be expressed as:

$$ {}^{t}PO_{K,x,y} = \left(\sum_{j=1}^{m-1} (W_j \times {}^{t}S_{j,x,y}) - W_m \times {}^{t}I_{K,x,y} \right) \times \prod_{r=1}^{R} {}^{t}EC_{r,x,y} \quad (5) $$

Specifically, both organic growth and spontaneous growth begin with seeds and grow through a moving window. First, the seed will be regarded as the center of the moving window, and a nonurban pixel in the neighborhood will be selected and converted to urban pixel according to the development probability (Equation 2) or potential (Equation 5) based on the roulette wheel method (Liu et al., 2012). Then, the window will be moved to center on the newly developed urban pixel, and the next nonurban pixel will be selected and converted in the same way. This step will be iterated until the neighborhoods are all occupied with urban pixels or the area of the urban growth patch meets the size demand (Equation 4), that is, to complete the simulation of a new urban growth patch. The urban expansion simulation will not be stopped until the total area of newly developed urban patches reaches the ULD. Referring to Chen et al. (2014), we set the moving window to 3*3 in size.

To ensure the validity of the urban expansion simulation results, the parameters of the LUSD-urban model need calibration through historical data. Referring to He et al. (2008), the adaptive Monte Carlo approach was adopted to automatically calibrate the weight parameters in the LUSD-urban model. In adaptive Monte Carlo, regional historical urban expansion will be repeatedly simulated with different parameters. Then, with an evaluation criterion of the kappa index, the simulation result closest to the actual situation will be found, and the corresponding weight parameters will be regarded as the best parameters of the model. Specifically, distance to city centers (with populations of less than 0.5, 0.5–1, 1–5, and more than 5 million), railways, highways, national roads, provincial roads, rivers, DEM, and slope data were taken as suitability factors. The land use/land cover data in 2015 were used as inherence factors. High-quality cropland and nature reserves were used as constrained factors. Then, 500 sets of parameters were produced based on adaptive Monte Carlo to simulate urban expansion from 2000 to 2010. The set of parameters with the highest kappa between the simulation result in 2010 and urban land data for 2010 was regarded as the best parameters for model calibration. The kappa of China's urban land in 2020 simulated by the patch-based LUSD-urban model after calibration was 0.69, indicating a relatively high accuracy. After that, we took urban land data for 2010 as initial input data, calibrated the model by using urban land data for 2020 in the same way, and then simulated future urban expansion in each province by using the calibrated model.

2.2.3. Delineation of UGB Based on the Simulation Results

Affected by complex terrain conditions and rapid urbanization, the urban landscape fragmentation of many regions in China tends to be high. In this case, the simulation results of urban land may be dispersed, which are unsuitable for restraining urban development and difficult to be directly used as UGBs. Following Liang et al. (2018), we combined morphological dilation and erosion and performed them to delineate UGBs (Figure 1b). The morphological method includes opening operations composed of erosion first and dilation followed and closing operations composed of dilation followed by erosion (Narayanan, 2006). The opening operation can remove fragmented urban patches, while the closing operation can bridge gaps between urban patches. The dilation algorithm uses a specific filter to move pixel by pixel on the image and assigns the maximum value among the image values covered by the filter to the central pixel in the filter. For the simulation results of future urban land classified as urban (1) and nonurban (0), the movement of the filter in dilation can convert its central nonurban pixel to an urban pixel. In contrast, the erosion algorithm assigns the minimum value in filter coverage to the central pixel in traversing the entire image. For the simulation results of future urban land, the movement of the filter in erosion can convert its central urban pixel to a nonurban pixel. The specific formulas of dilation and erosion can be found in Liang et al. (2018). Specifically, referring to Liang et al. (2018), the closing operation was first executed to connect adjacent urban patches and then the opening operation was executed to remove some isolated tiny patches to delineate UGBs by using a filter with removal of four pixels at corners. As shown in Figure 1b, the delineation results of UGBs processed by morphological dilation and erosion can be more consistent with the rules and the actual situation of urban expansion, for example, newly developed urban patches must be connected to existing urban patches through roads and other infrastructures. To ensure the boundaries are continuous and smooth while close to the urban outline, the filter was defined as 3*3 in size referring to Chen et al. (2014).

2.3. Estimation of Pressures From Urban Shrinkage

With the socioeconomic recession, urban shrinkage began to appear (Haase, Rink, et al., 2014; Haase et al., 2016; Yang & Dunford, 2018), usually manifesting in urban population decline (Kroll & Kabisch, 2012), urban housing vacancies (Wang et al., 2020) and existing urban infrastructure idling (Haase, Rink, et al., 2014; Sousa & Pinho, 2015). In view of massive urban shrinkage in China, which had been a stress for urban sustainability (Yang et al., 2021), and the pressure from future urban shrinkage in each province was still unclear, we evaluated the

future pressure from urban shrinkage at the provincial level from 2021 to 2100 under five SSPs following the method adopted by Chen, Li, et al. (2020). Referring to Long and Wu (2016), we assumed that the impacts of other driving factors, such as economic depression, will be first reflected in population decline, and then affect the urban land demand. Thus, urban shrinkage pressure can be defined as the percentage of unnecessary ULA relative to the urban population in 2100 to the extent of UGB (i.e., the ULA when the urban population peaked) (Chen, Li, et al., 2020). The pressure can be expressed as:

$$PR_{i,s,T} = \frac{A_{i,s,T}^{UGB} - A_{i,s}^{2100}}{A_{i,s,T}^{UGB}} \times 100\% \tag{6}$$

$$A_{i,s}^{2100} = \beta_{0i} + \beta_{1i} \times UP_{i,s}^{2100} + \varepsilon_{i,s} \tag{7}$$

where $PR_{i,s,T}$ refers to the urban shrinkage pressure of province i under scenario s and urban expansion mode T. $A_{i,s,T}^{UGB}$ and $A_{i,s}^{2100}$ refer to the extent of the UGB of province i under scenario s and urban expansion mode T and the ULD of province i under scenario s in 2100, respectively. $A_{i,s}^{2100}$ can be calculated according to Equation 7, where $UP_{i,s}^{2100}$ refers to the urban population in 2100 of province i under scenario s.

2.4. Evaluating the Effects of Urban Expansion on Ecosystem Services

Ecosystem services are the foundation for human well-being and sustainable development, including supporting services, provisioning services, regulating services, and cultural services (Millennium Ecosystem Assessment, 2005; Wu, 2013, 2021). Land use/cover change, population growth, and economic growth owing to rapid urban expansion all affect and change ecosystem services directly and indirectly. Therefore, understanding the impacts of urban expansion on ecosystem services is crucial for urban sustainability. In this study, we adopted habitat quality in supporting services, food production in provisioning services and carbon sequestration in regulating services as examples and evaluated the possible impacts of future urban expansion on ecosystem services under different scenarios and diverse urban expansion modes.

In this study, we quantified the spatial pattern of habitat quality in China by using the Habitat Quality module in the Integrated Valuation of Ecosystem Services and Trade-offs (InVEST) model (Sharp et al., 2016; Song et al., 2020). Then, following Sun et al. (2017), we allocated the provincial total grain output, obtained from the China Statistical Yearbook (http://www.stats.gov.cn/), to cropland pixels according to NPP data and land use/land cover data and calculated the spatial distribution of food production. With reference to Meng et al. (2018), we took NPP to represent the level of carbon sequestration. Specific calculation formulas and parameters for each ecosystem service were shown in (Texts S1–S3 in Supporting Information S1). The impacts of urban expansion on ecosystem services were evaluated based on the simulation results of future urban expansion and the ecosystem services at the baseline of 2020. The equation can be expressed as:

$$S_{i,s,T}^{loss} = \sum_{x,y}{}^{x,y}ES_{i,s,T}\left({}^{x,y}Urban_{i,s,T}^{UGB} - {}^{x,y}Ubran_{i}^{2020}\right) \tag{8}$$

where $S_{i,s,T}^{loss}$ refers to the ecosystem service loss of province i under scenario s and urban expansion mode T. ${}^{x,y}ES_{i,s,T}$ refers to the assessed value of ecosystem service in pixel (x,y) of province i. ${}^{x,y}Urban_{i,s,T}^{UGB}$ refers to whether pixel (x,y) of province i is within UGBs under scenario s and urban expansion mode T for 2021–2100, with 0 representing outside the UGB and 1 representing within the UGB. ${}^{x,y}Ubran_{i}^{2020}$ refers to the classification value of urban land in pixel (x,y) of province i in 2020, with 0 representing nonurban land and 1 representing urban land.

3. Result

3.1. Future Urban Land Demand

The ULD in China from 2021 to 2100 was projected to increase first and then decrease (Figure 2a). China's ULD was projected to peak at 111,879–115,827 km^2 in 2042–2048, with an increase of 23.82–28.19% compared with ULA in 2020 (Table 2). The decline in China's ULD after peaking significantly was projected to differ under

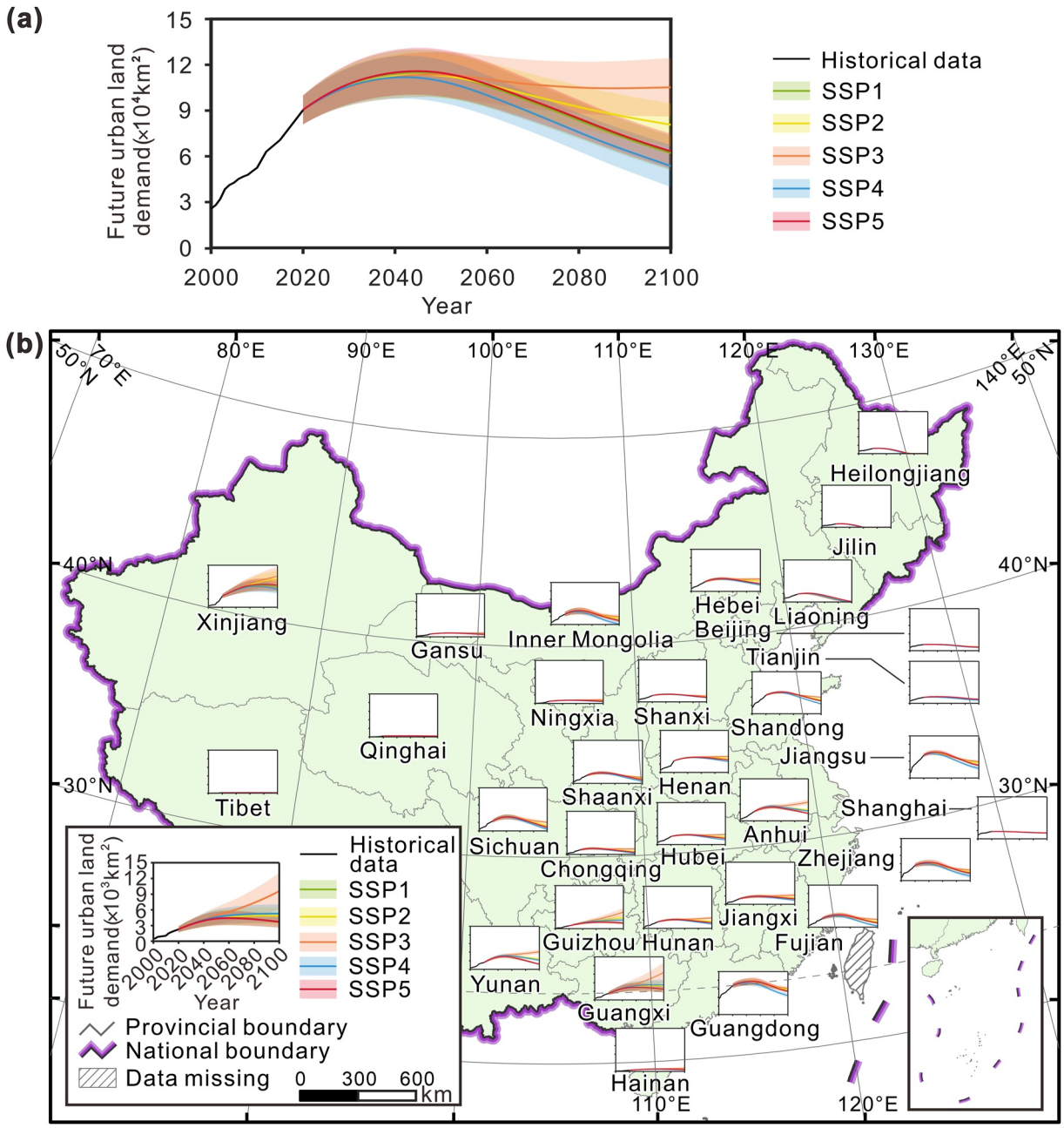

Figure 2. Future urban land demand in China (a) and provinces (b). *Note.* The shaded areas indicate the 95% confidence intervals of the estimated urban land demand in each province. The 95% confidence intervals of China were obtained from the sum of provinces.

different scenarios. SSP1 is a green growth pathway, or a sustainable development pathway, under which the ULD was projected to decrease by 42.79%, from 115,093 km^2 in 2044 to 65,850 km^2 in 2100. SSP2 is a middle pathway, which can be comprehended as a pathway following the historical development trajectory. Under SSP2, ULD was projected to decrease by 26.07%, from 113,597 km^2 in 2046 to 83,979 km^2 in 2100. Under SSP3, a regional rivalry pathway with large regional development gaps, the decline will be minimal, with ULD dropping from 113,668 km^2 in 2048 to 108,712 km^2 in 2100, decreasing by 4.36%. ULD will experience the most dramatic decline under SSP4, a highly unequal development pathway within and across countries, which was projected to decrease by 48.04%, dropping from 111,879 km^2 in 2042 to 58,128 km^2 in 2100. SSP5 is a fossil fuel development pathway that emphasizes a traditional, economic development-oriented way to solve socioeconomic

Table 2
Maximum Urban Land Demand From 2021 to 2100 of China in Provinces

Provinces	Urban land area in 2020/km^2	Maximum urban land demand from 2021 to 2100/km^2 (corresponding year)				
		SSP1	SSP2	SSP3	SSP4	SSP5
Beijing	2,181	2,239(2030)	2,241(2029)	2,239(2029)	2,231(2029)	2,251(2031)
Tianjin	2,105	2,221(2035)	2,223(2034)	2,191(2032)	2,201(2032)	2,389(2039)
Hebei	3,459	4,564(2045)	4,511(2048)	4,469(2051)	4,477(2043)	4,572(2045)
Shanxi	2,250	2,744(2044)	2,689(2044)	2,660(2046)	2,723(2043)	2,750(2044)
Inner Mongolia	3,662	4,912(2042)	4,806(2041)	4,707(2041)	4,557(2037)	4,943(2042)
Liaoning	2,790	3,094(2034)	3,040(2032)	2,970(2029)	3,062(2033)	3,152(2035)
Jilin	1,186	1,263(2027)	1,267(2027)	1,266(2027)	1,248(2026)	1,264(2027)
Heilongjiang	1,826	1,936(2029)	1,931(2028)	1,920(2027)	1,918(2028)	1,934(2029)
Shanghai	2,618	2,632(2025)	2,632(2025)	2,632(2024)	2,630(2024)	2,634(2026)
Jiangsu	8,120	9,160(2036)	8,896(2034)	8,768(2033)	8,757(2032)	9,222(2037)
Zhejiang	5,439	6,319(2040)	6,164(2037)	6,044(2037)	6,032(2035)	6,425(2041)
Anhui	3,271	5,032(2047)	5,002(2050)	6,717(2100)	5,151(2048)	4,944(2046)
Fujian	3,120	4,345(2045)	4,207(2044)	4,165(2046)	3,977(2039)	4,399(2045)
Jiangxi	2,023	2,896(2048)	2,842(2050)	3,254(2100)	2,797(2045)	2,873(2048)
Shandong	6,625	7,740(2042)	7,573(2041)	7,474(2041)	7,567(2039)	7,763(2043)
Henan	4,179	5,471(2051)	5,463(2057)	5,704(2100)	5,340(2048)	5,448(2052)
Hubei	2,877	3,517(2045)	3,468(2046)	3,581(2049)	3,425(2042)	3,495(2045)
Hunan	2,291	3,195(2047)	3,152(2049)	3,722(2100)	3,099(2045)	3,164(2047)
Guangdong	10,095	11,492(2048)	11,372(2048)	11,270(2048)	11,019(2040)	11,616(2049)
Guangxi	2,293	4,498(2061)	4,912(2088)	9,583(2100)	5,287(2098)	4,426(2061)
Hainan	424	809(2060)	878(2086)	1,150(2100)	773(2056)	828(2060)
Chongqing	1,621	2,085(2038)	2,034(2038)	2,032(2043)	2,052(2037)	2,077(2038)
Sichuan	3,453	4,963(2042)	4,831(2042)	4,760(2043)	4,849(2040)	4,922(2042)
Guizhou	986	2,339(2067)	3,752(2100)	5,788(2100)	2,973(2099)	2,294(2069)
Yunnan	2,402	4,479(2048)	4,699(2053)	6,119(2100)	4,772(2052)	4,490(2048)
Tibet	153	199(2058)	201(2060)	207(2068)	199(2063)	203(2062)
Shaanxi	2,869	3,731(2041)	3,605(2040)	3,533(2040)	3,640(2039)	3,737(2042)
Gansu	978	1,339(2049)	1,354(2052)	1,381(2057)	1,362(2049)	1,334(2048)
Qinghai	335	409(2048)	411(2051)	412(2051)	404(2046)	413(2050)
Ningxia	748	1,117(2054)	1,134(2057)	1,326(2100)	1,091(2048)	1,146(2053)
Xinjiang	3,974	7,795(2075)	10,082(2100)	11,072(2100)	7,470(2070)	8,149(2082)
China	90,353	115,093(2044)	113,597(2046)	113,668(2048)	111,879(2042)	115,827(2045)

problems through the pursuit of self-interest. The changing trend under SSP5 was similar to SSP1 with ULD decreasing by 42.19%.

There were differences in the future ULD in provinces (Figure 2b and Table 2). The ULD of seven provinces, including Beijing, Shanghai, Tianjin, Heilongjiang, Jilin, Liaoning, and Tibet, was projected to rise to a high point first and then decrease, with no significant difference in the decline of ULD under different scenarios. Thirteen provinces, including Jiangsu, Zhejiang, Fujian, Guangdong, Chongqing, Sichuan, Hebei, Inner Mongolia, Shanxi, Shandong, Shaanxi, Gansu, and Qinghai, were projected to show a similar trend, with the ULD increasing followed by a decrease, and the differences in the decline of the ULD under the five SSPs can be found. The trend of ULD in the provinces of Henan, Anhui, Hubei, Hunan, Jiangxi, Guizhou, Guangxi, Hainan, Yunnan, Ningxia, and Xinjiang was projected to significantly differ under the five SSPs. Among these 11 provinces, the

ULD of Guizhou and Xinjiang was projected to continuously increase under SSP2 and SSP3, and the ULD of other provinces was projected to continuously increase under SSP3, while the ULD was projected to show a trend of increasing first and then decreasing under other scenarios from 2021 to 2100.

3.2. Spatial Patterns of UGBs

There were differences in the extent of UGBs in China under five scenarios from 2021 to 2100 (Figure 3a and Table 3). Under SSP3, the extent of UGBs will be largest, in the range of 137,309–142,982 km^2 under 11 urban expansion modes, which was projected to be 46,956–52,629 km^2 (51.97–58.25%) larger than the ULA in 2020. The extent of UGBs in China under other scenarios will be similar, in the range of 121,199–129,668 km^2, which was projected to be 30,846–39,315 km^2 (34.13–43.51%) larger than the ULA in 2020.

For five provinces, including Anhui, Guizhou, Guangxi, Yunnan, and Xinjiang, the area of urban land to be expanded within UGBs was projected to be huge and significantly differ under the five scenarios (Figure 3b, Table 3 and Table S3–S7 in Supporting Information S1). Under SSP3, the extent of UGBs in these five provinces will be larger than that under other scenarios. For example, in Guangxi, the area of urban land to be expanded within UGBs was projected to be 8,096–8,879 km^2 under SSP3, which was 353.07–387.22% of the ULA in 2020, while under other scenarios, the area was projected to be 2,227–3,732 km^2 (97.12–162.76%). For other provinces, no significant difference was found in the area of urban land to be expanded within UGBs under different scenarios. Among these provinces, the area of urban land to be expanded within UGBs will be mainly larger than 1,500 km^2 for Henan, Guangdong and Sichuan and will be mainly between 1,000 and 1,500 km^2 for six provinces, including Hebei, Inner Mongolia, Jiangsu, Zhejiang, Fujian, and Shandong and will be mainly between 500 and 1,000 km^2 for Shanxi, Hubei, Hunan, Jiangxi, Chongqing, and Shaanxi and will be less than 500 km^2 for the remaining 11 provinces.

For 17 cities with more than 5 million people, the extent of UGBs was projected to have no obvious difference under the five scenarios (Figure 3c, Tables S8–S12 in Supporting Information S1) but differ under diverse urban expansion modes (Figure 4). The area of land to be expanded within the UGBs of Chengdu, Hangzhou, and Chongqing was projected to be large. For six cities, including Guangzhou, Tianjin, Chengdu, Hangzhou, Nanjing, and Jinan, the extent of UGBs under spontaneous growth will be larger than that under organic growth, while in the six provinces of Shenzhen, Dongguan, Wuhan, Zhengzhou, Shenyang, and Suzhou, such a difference will be reversed. The extent of UGBs in Beijing and Xi'an was projected to have no obvious regularity under different urban expansion modes.

3.3. Pressure of Future Urban Shrinkage

China will face urban shrinkage pressure under all SSPs (Figure 5a, Tables S13–S17 in Supporting Information S1). Under SSP4, China will face the most severe urban shrinkage pressure, with ULD in 2100 dropping to 58,128 km^2, a decrease of 52.04–53.41% compared with the UGB area of 121,199–124,752 km^2. Under SSP1 and SSP5, China's ULD in 2100 will decrease by 45.68–47.91%. This value was projected to be 32.99–35.24% under SSP2. Under SSP3, China will face the smallest urban shrinkage pressure. The ULD of China was projected to drop to 108,712 km^2, decreasing by 20.83–23.97% compared with the UGB area of 137,309–142,982 km^2.

As shown in Figure 5b, Heilongjiang, Jilin, and Liaoning will face remarkable urban shrinkage pressure, with a decrease of more than 90% in ULA under five scenarios and 11 urban expansion modes. In Beijing and Tianjin, the ULA was projected to decline by 35.57–52.40%. Shanghai, Henan, Guizhou, Guangdong, Guangxi, Xinjiang, and Tibet will face relatively low urban shrinkage pressure under all scenarios and urban expansion modes, with a decreasing rate of less than 32.00%. These 12 provinces will encounter similar urban shrinkage pressures under the five scenarios.

The urban shrinkage pressure in the other provinces was projected to have significant differences under the five SSPs. Hainan will face smaller pressure under SSP2 and SSP3. 18 provinces, including Hebei, Hubei, and Yunnan, will face less pressure under SSP3, with substantial urban shrinkage pressure under other scenarios. For example, in Yunnan, the ULD will continue to increase under SSP3, with an urban shrinkage pressure of 0.00–3.65%, whereas under SSP1 and SSP5, the ULD will decline after peaking in 2066 and 2048, respectively. Compared with the extent of UGBs, the decline proportion of ULD in 2100 was projected to be as high as

10.1029/2021EF002572

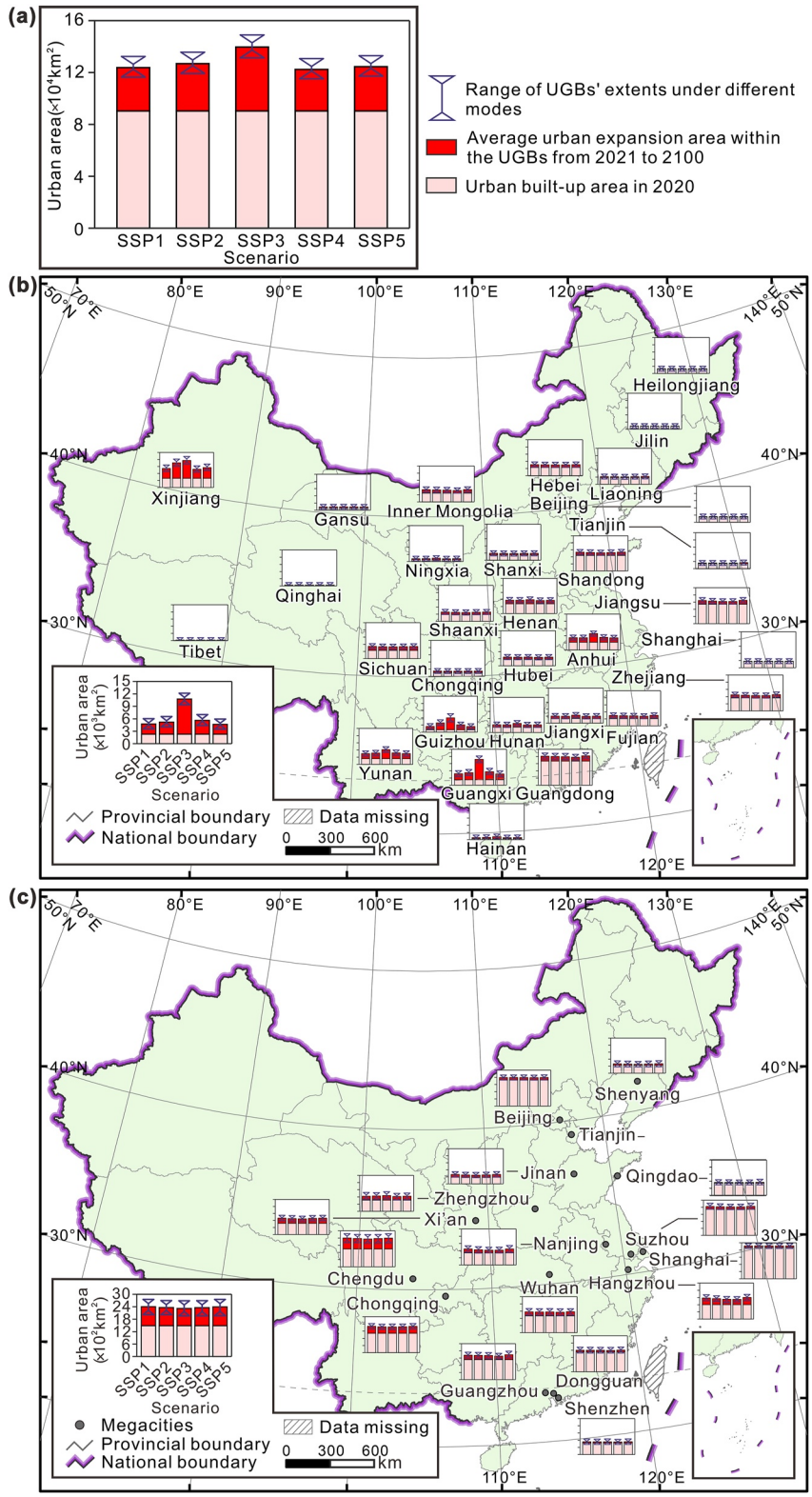

Figure 3. Extent of urban growth boundaries in China (a), provinces (b), and major cities (c).

Table 3
Extent of Urban Growth Boundaries in Provinces From 2021 to 2100

Provinces	Urban land area in 2020/km^2	Extent of urban growth boundaries under different urban expansion modes from 2021 to 2100/km^2				
		SSP1	SSP2	SSP3	SSP4	SSP5
Beijing	2,181	2,375–2,397	2,378–2,403	2,375–2,402	2,375–2,390	2,384–2,412
Tianjin	2,105	2,341–2,399	2,352–2,406	2,319–2,364	2,321–2,374	2,521–2,578
Hebei	3,459	4,572–4,736	4,503–4,646	4,457–4,611	4,484–4,620	4,515–4,726
Shanxi	2,250	2,838–2,966	2,769–2,890	2,755–2,852	2,808–2,920	2,848–2,952
Inner Mongolia	3,662	5,018–5,260	4,913–5,141	4,833–5,049	4,674–4,857	5,069–5,287
Liaoning	2,790	3,220–3,250	3,159–3,216	3,110–3,138	3,189–3,223	3,264–3,313
Jilin	1,186	1,284–1,321	1,294–1,313	1,289–1,309	1,275–1,292	1,293–1,309
Heilongjiang	1,826	2,001–2,043	1,990–2,035	1,980–2,037	1,981–2,029	1,998–2,044
Shanghai	2,618	2,740–2,752	2,742–2,752	2,738–2,753	2,739–2,748	2,738–2,756
Jiangsu	8,120	9,577–9,853	9,334–9,537	9,209–9,377	9,191–9,383	9,639–9,878
Zhejiang	5,439	6,661–6,816	6,491–6,635	6,377–6,501	6,373–6,508	6,754–6,934
Anhui	3,271	5,121–5,232	5,080–5,223	6,809–6,911	5,240–5,364	5,034–5,145
Fujian	3,120	4,413–4,543	4,312–4,419	4,234–4,332	4,080–4,180	4,464–4,553
Jiangxi	2,023	2,942–3,134	2,878–3,081	3,323–3,528	2,842–3,010	2,934–3,097
Shandong	6,625	7,958–8,145	7,812–7,998	7,713–7,864	7,802–7,945	8,004–8,170
Henan	4,179	5,659–5,843	5,616–5,807	5,807–6,091	5,514–5,685	5,603–5,758
Hubei	2,877	3,662–3,836	3,607–3,766	3,670–3,823	3,553–3,715	3,646–3,815
Hunan	2,291	3,232–3,478	3,177–3,428	3,752–4,104	3,127–3,377	3,183–3,444
Guangdong	10,095	11,887–12,433	11,798–12,302	11,713–12,239	11,469–11,901	12,020–12,571
Guangxi	2,293	4,585–5,030	5,043–5,541	10,389–11,172	5,393–6,025	4,520–4,959
Hainan	424	792–908	862–997	1,138–1,337	754–866	811–939
Chongqing	1,621	2,183–2,234	2,148–2,181	2,126–2,188	2,153–2,191	2,181–2,229
Sichuan	3,453	5,036–5,270	4,929–5,101	4,869–5,066	4,931–5,122	5,019–5,209
Guizhou	986	2,354–2,568	3,730–4,145	5,187–6,716	2,959–3,197	2,320–2,512
Yunnan	2,402	4,378–4,623	4,606–4,831	6,011–6,351	4,691–4,939	4,390–4,646
Tibet	153	195–214	200–219	203–225	193–210	193–220
Shaanxi	2,869	3,844–3,977	3,722–3,833	3,653–3,781	3,745–3,891	3,847–3,941
Gansu	978	1,367–1,411	1,374–1,424	1,412–1,441	1,382–1,425	1,361–1,408
Qinghai	335	400–417	396–431	398–416	396–415	402–420
Ningxia	748	1,174–1,224	1,204–1,231	1,384–1,448	1,145–1,195	1,217–1,242
Xinjiang	3,974	7,898–8,646	10,108–11,168	11,050–12,267	7,541–8,273	8,247–9,046
China	90,353	122,513–126,427	125,321–129,668	137,309–142,982	121,199–124,752	123,270–126,959

59.04–61.88%, resulting in remarkable urban shrinkage pressure. Nine provinces, including Inner Mongolia, Ningxia, Shaanxi, Shandong, Jiangsu, Zhejiang, Fujian, Sichuan, and Chongqing, will face more severe urban shrinkage pressure under SSP4. For example, in Inner Mongolia, ULD in 2100 was projected to decrease by 97.92–98.00% compared with the extent of UGBs.

3.4. Occupancy of Urban Expansion Within UGBs on Other Land Use/Cover Types

Future urban expansion in China will mainly occupy cropland (Figure 6a). By 2100, 43.28–47.04% of newly developed urban land in China was projected to be converted from cropland. Rural residential areas and other construction land were projected to collectively contribute to 14.91–18.71% of newly developed urban land.

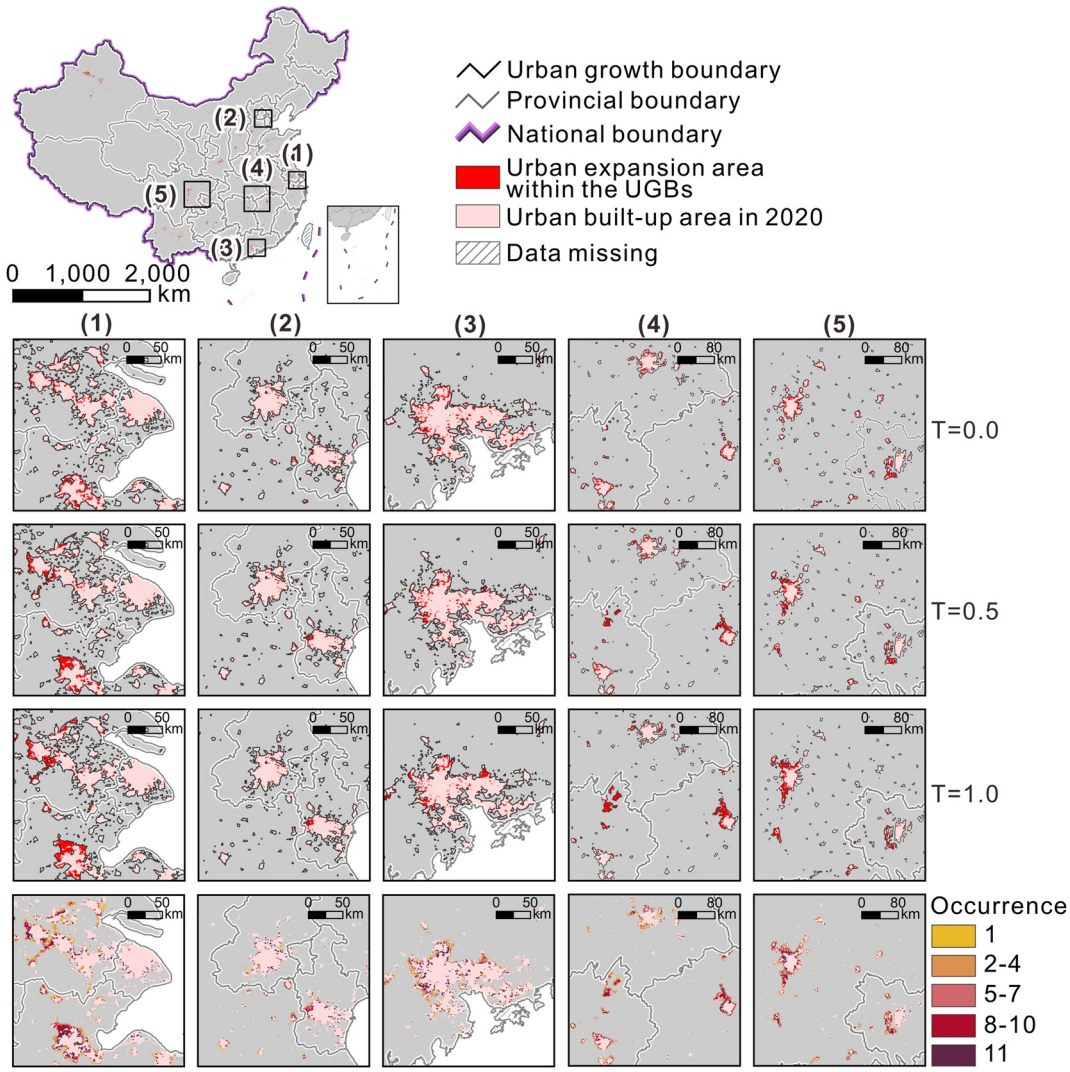

Figure 4. Spatial pattern of urban growth boundaries in China under shared socioeconomic pathway 1 (SSP1). *Note.* (1) represents the Yangtze River Delta Urban Agglomeration; (2) represents the Beijing-Tianjin-Hebei Urban Agglomeration; (3) represents the Guangdong-Hong Kong-Macao Greater Bay Area; (4) represents the urban agglomeration in the middle reaches of the Yangtze River; (5) represents the Chengdu-Chongqing Urban Agglomeration. Occurrence refers to the frequency of pixels within urban growth boundaries under 11 urban expansion modes.

Forest and grassland were projected to account for 11.40–17.11% and 12.19–14.39% of newly developed urban land, respectively. Wetland and bare land were projected to represent 5.75–7.06% and 3.15–5.23% of newly developed urban land, respectively.

There were significant differences in the occupancy of future urban expansion on other land use/cover types in provinces (Figure 6b and Figures S1–S4 in Supporting Information S1). Taking the SSP1 scenario as an example, for Hunan, Jiangxi, Guangxi, Chongqing, and Hainan, cropland and forest will be the main sources of newly developed urban land, collectively accounting for 68.56–84.17%. This was evident in the case of Hunan, where 39.53–44.06% and 31.56–39.02% of newly developed urban land were projected to be converted from cropland and forest, respectively. In Inner Mongolia and Yunnan, cropland and grassland were projected to be the main sources of newly developed urban land. In Hubei, Heilongjiang, and Ningxia, apart from cropland with the largest proportion, wetland, rural residential area, and other construction land will represent an even proportion. For example, in Hubei, 49.68–54.54% of newly developed urban land was projected to be converted from cropland, and 18.87–24.94% and 17.50–20.57% of newly developed urban land were projected to be made up of wetland and rural residential area and other construction land, respectively. In Guangdong and Fujian, apart from cropland

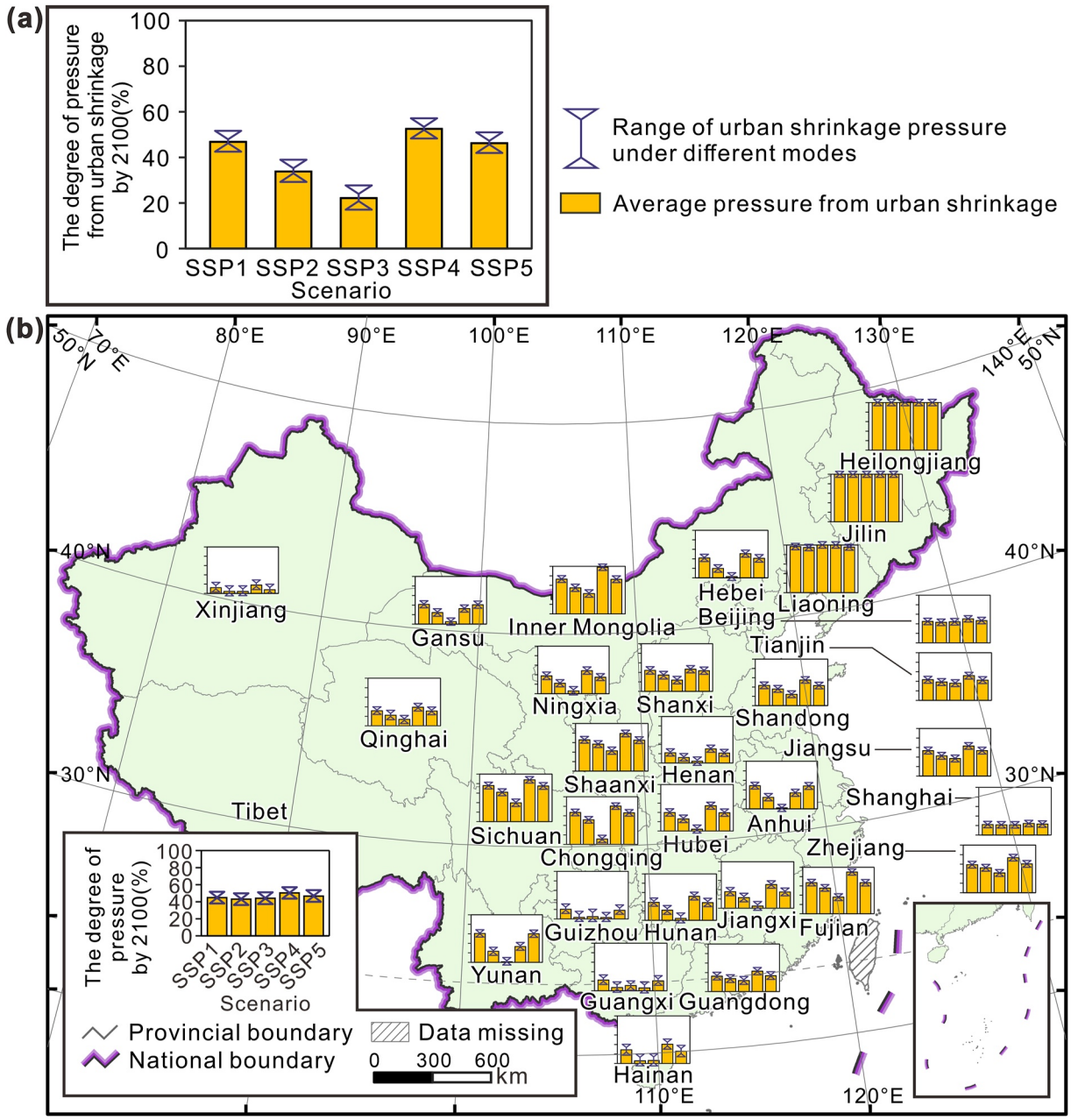

Figure 5. Future urban shrinkage pressure in China (a) and provinces (b).

with the largest proportion, forest, and rural residential areas and other construction land will represent an even proportion. In Gansu and Xinjiang, grassland and bare land were projected to be the main sources of newly developed urban land. For example, in Tibet, grassland and wetland were projected to collectively contribute to 63.04–76.00% of newly developed urban land. In Qinghai, cropland, grassland, rural residential area, and other construction land were projected to occupy evenly, while in Guizhou, cropland, forest, and grassland were projected to account for an even proportion. In the remaining 14 provinces, including Beijing, Tianjin, and Hebei, cropland and rural residential areas and other construction land will be the main sources of newly developed urban land (75.62–96.15%, collectively), while other land use/cover types will constitute a relatively low proportion.

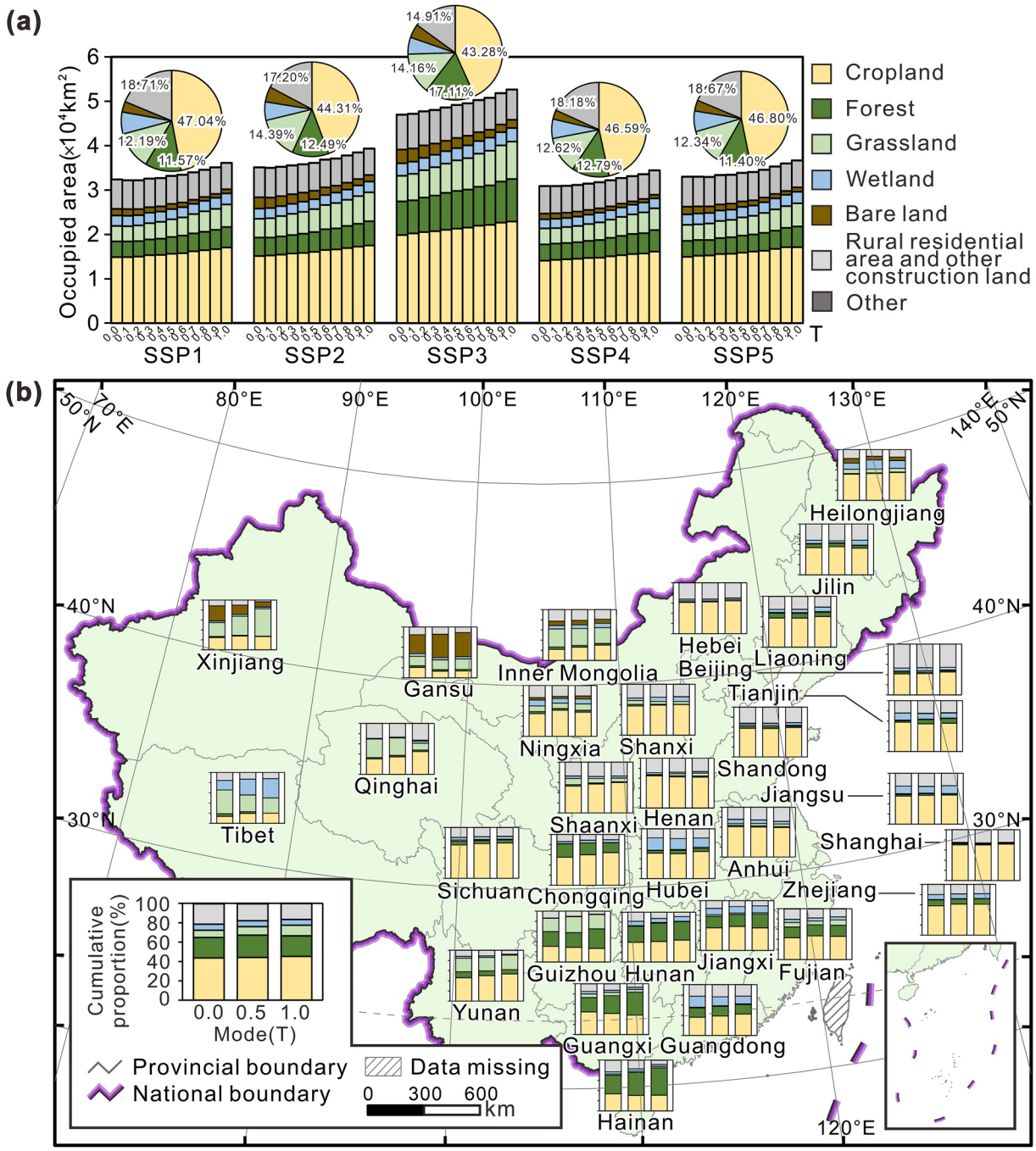

Figure 6. Occupancy of future urban expansion on other land use/cover types in China (a) and provinces under shared socioeconomic pathway 1 (SSP1) (b).

3.5. Effects of Urban Expansion Within UGBs on Ecosystem Services

Urban expansion in China will cause a simultaneous decline in habitat quality, food production, and carbon sequestration (Figure 7a). Under SSP3, urban expansion was projected to cause the most severe negative impacts on ecosystem services, with habitat quality decreasing by 0.40–0.43%, food production decreasing by 0.75–0.97%, and carbon sequestration decreasing by 0.53–0.69%. Under SSP4, urban expansion will lead to the smallest losses of habitat quality, food production, and carbon sequestration, decreasing by 0.26–0.28%, 0.51–0.67%, and 0.32–0.42%, respectively. For six provinces, including Tianjin, Anhui, Guizhou, Guangxi, Hainan, and Xinjiang, the losses of three ecosystem services were projected to have significant differences under five scenarios. Among

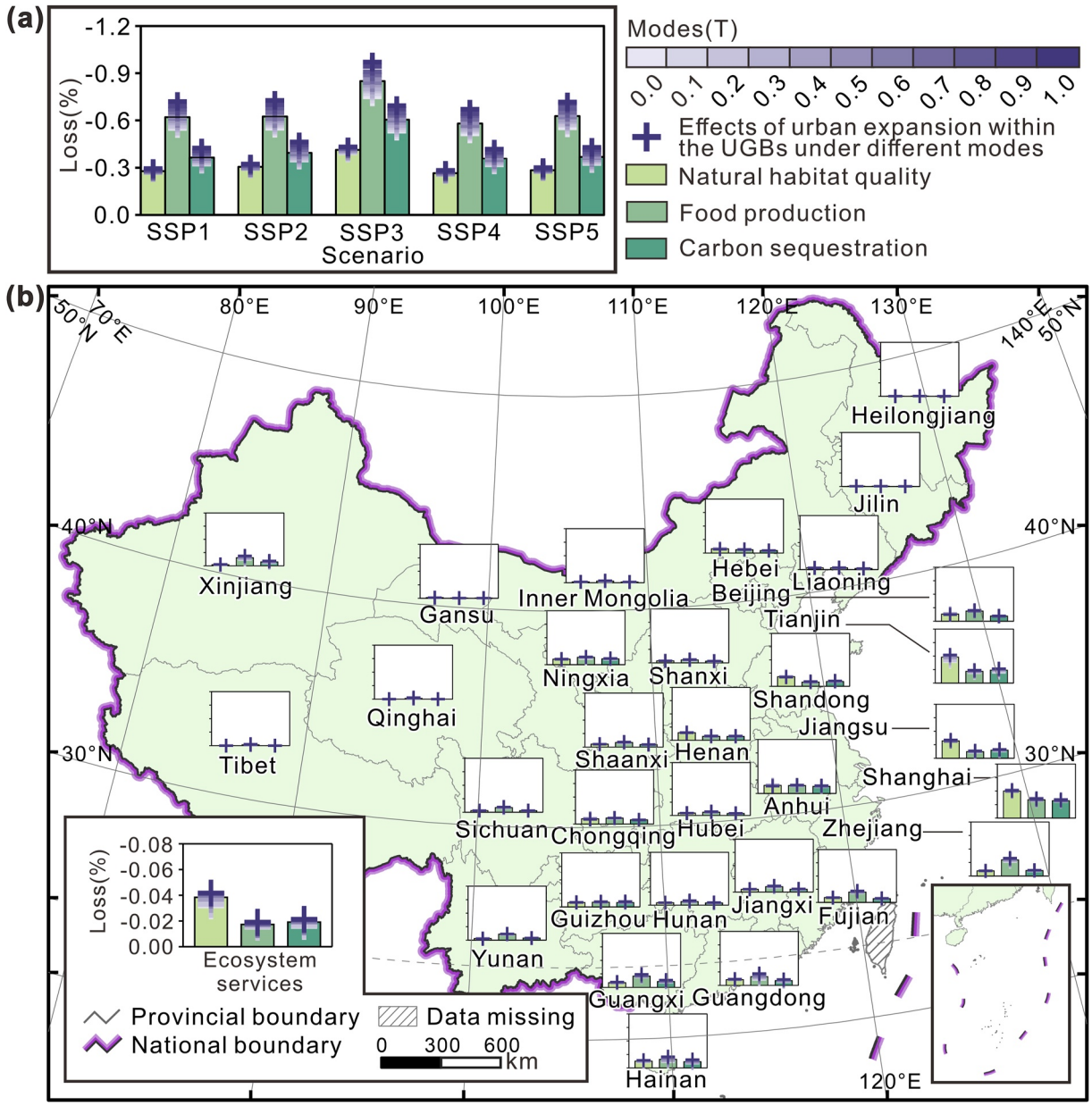

Figure 7. Effects of future urban expansion on ecosystem services in China (a) and provinces under shared socioeconomic pathway 1 (SSP1) (b).

these provinces, five provinces, including Anhui, Guizhou, Guangxi, Hainan, and Xinjiang, will suffer from more severe ecosystem service losses under SSP3, while the ecosystem service losses of Tianjin under SSP5 will be higher than those under other scenarios (Figure 7b and Figures S5–S8 in Supporting Information S1).

For the same scenario, urban expansion under spontaneous growth will lead to greater losses of ecosystem services than that under organic growth (Figure 7a). For example, under SSP1, urban expansion under organic growth ($T = 0.0$) will cause a decrease in habitat quality, food production, and carbon sequestration by 0.28%, 0.55%, and 0.32%, respectively. urban expansion under spontaneous growth ($T = 1.0$) will lead to habitat quality, food production and carbon sequestration dropping by 0.29%, 0.72%, and 0.43%, respectively. In 10 provinces, including Hebei, Tianjin, Shanghai, Zhejiang, Anhui, Guizhou, Guangxi, Guangdong, Hainan, and Xinjiang, the losses of ecosystem services were projected to show significant differences under diverse urban expansion modes. Compared with the urban expansion modes dominated by organic growth ($T < 0.5$), the urban expansion

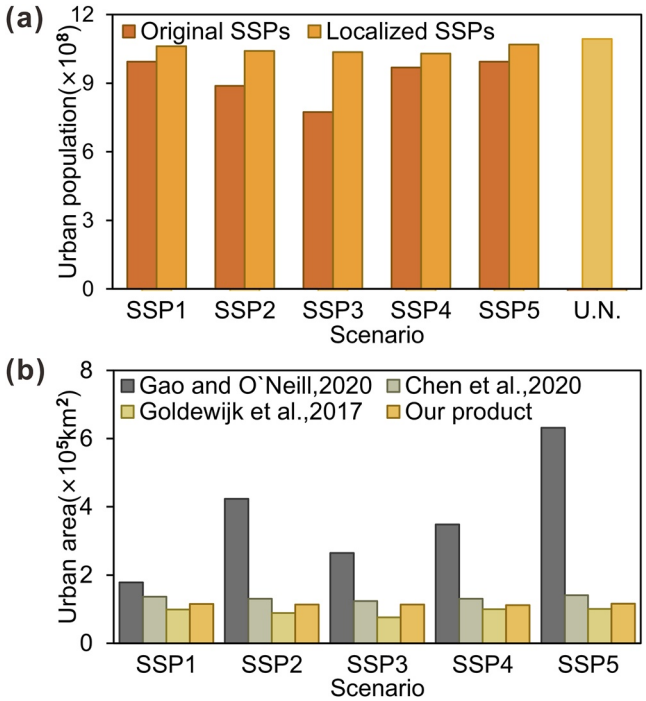

Figure 8. Comparison of simulation results of urban population (a) and urban land demand (b). *Note.* In Figure 8a, the values of the original shared socioeconomic pathways (SSPs) and the localized SSPs represent the maximum urban population of China by 2100. The values of the U.N. data set represent the maximum urban population of China by 2050.

modes dominated by spontaneous growth ($T > 0.5$) will lead to more severe losses of ecosystem services (Figure 7b and Figures S5–S8 in Supporting Information S1).

4. Discussion

4.1. Comparison With Existing Studies

We first compared the simulation results of the urban population from the original SSPs, localized SSPs and the United Nations (U.N.) data set (https://population.un.org/wpp/) (Figure 8a). Under the five scenarios, the urban population under localized SSPs was larger than that under the original SSPs and was closer to the urban population given by the U.N. data set. Without taking the adjustment of family planning policies into consideration, this was a possible explanation for the underestimation of the future urban population in China (Chen, Guo, et al., 2020; Jiang et al., 2017). In addition, provincial population and urban share with consideration of the differences in socioeconomic development of different provinces were provided by localized SSPs. Therefore, more comprehensive and reliable information was provided by the original SSPs.

Then, we compared the simulated future urban land with three published urban land products (Figure 8b). These three urban land products all simulate global urban expansion by 2100 based on original SSPs. The first one is from Gao and O'Neill (2020) at a 0.125-degree spatial resolution. The second data set is from Chen, Li, et al. (2020), with a spatial resolution of 1 km. The third data set is the HYDE data set from Goldewijk et al. (2017) featuring a spatial resolution of 0.083°. The ULD given by Goldewijk et al. (2017) is smaller than our product, which is consistent with a lower urban population estimation result under the original SSPs, while the ULD from Gao and O'Neill (2020) and Chen, Li, et al. (2020) are generally larger than that from our product. Failing to distinguish urban and rural land in these two data sets is the main reason for overestimation of future ULD (Figure 9). Furthermore, ULD in different provinces was used in our work to simulate future urban expansion under 11 modes. Compared with the simulation results based only on the national ULD and single urban expansion mode, the provincial simulation results in this study were more reliable and can fully demonstrate the possibility of future urban spatial patterns in each province.

4.2. Similarities and Differences in Future Urban Growth Across Provinces

For Beijing, Tianjin, Shanghai, Heilongjiang, Jilin, Liaoning, and Tibet, there is no obvious difference in the urban land dynamics and there is a slight expansion of urban land within the UGBs under each SSP scenario (Figures 2 and 3). This can be related to the limited urban population growth in these provinces. Among them, three provinces including Beijing, Tianjin, and Shanghai with higher economic level have stepped into a relatively mature stage. Relatively strict household registration policies and population ceiling restrictions of megacities may lead to a slight population increase in these provinces. Differently, in Heilongjiang, Jilin, and Liaoning, three provinces in northeast China, a series of development problems have occurred on account of the heavy industrial structure, slow development of the private economy and natural resources depletion, since the reform and opening up in 1978 (Sun & Wang, 2021). In addition to the urban middle-aged labor forces have continued to lose recently and the aging population structure has deepened (Yang, 2019), the economic development has become sluggish and the urban growth vitality has lacked in northeast China. This might explain why urban land demand continues to decline after a temporary rise in these three provinces. Limited by the natural conditions, Tibet, on the other hand, has a relatively low urban development level and relatively slow urbanization process, and thus was less influenced by different scenarios.

For five provinces including Anhui, Guizhou, Guangxi, Yunnan, and Xinjiang, the urban land demand continues to increase under SSP3 and the urban area within UGBs is much larger than those under other SSP scenarios

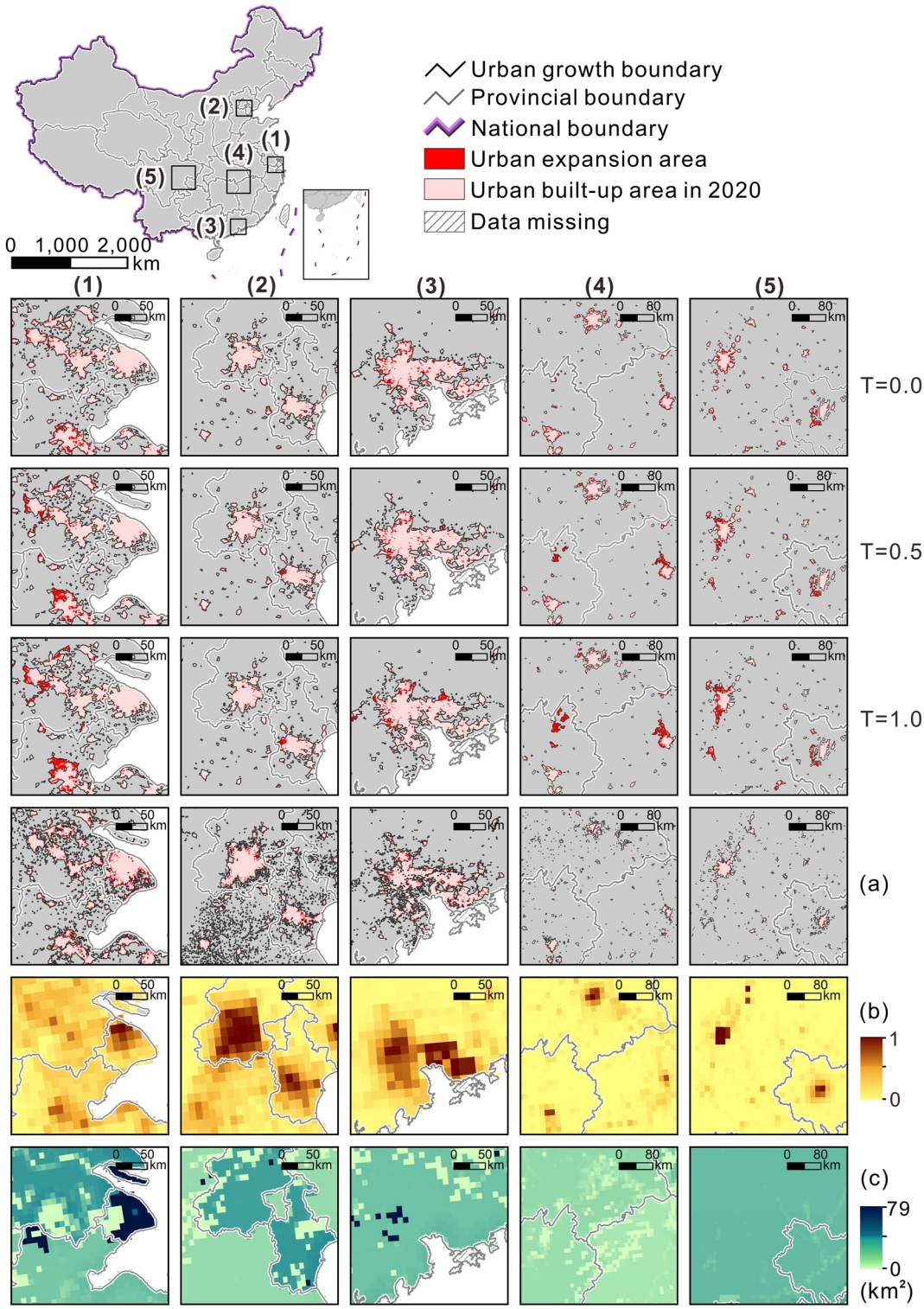

Figure 9. Comparison of simulation results of urban land spatial patterns. *Note.* (a) Refers to the product from Chen, Li, et al. (2020), (b) refers to the product from Gao and O'Neill (2020), ranging from 0 to 1 to represent the proportion of urban land in pixels. (c) refers to the product from Goldewijk et al. (2017), representing the urban land area in pixels.

(Figures 2 and 3). These provinces are located in central-western China, with relatively low economic development level and relatively high fertility rate. Under SSP3, a regional rivalry scenario, the already higher fertility rates in these provinces were projected to be further amplified (Chen, Guo, et al., 2020), and thus the number of newborns will increase rapidly. Meanwhile, the local population was projected to keep rising because of the relatively low migration rates (Chen et al., 2022). This has led to an increase in urban land demand and continuous urban expansion as the population grows. The continuously rising urban land demand in the six provinces of Hubei, Hunan, Jiangxi, Henan, Hainan, and Ningxia under SSP3 can also be explained by the above reasons (Figure 2).

In Jiangsu, Zhejiang, Fujian, Shandong, and Guangdong, the urban area expected to expand within the UGBs was large and there was no significant difference under five scenarios. But the descent range of urban land demand thereafter varied with scenarios and was projected to be the largest under SSP4. This can be explained by the generally lower urban population growth resulting from the population development pattern with low fertility rates and moderate mortality rates under SSP4 (Chen, Guo, et al., 2020). A similar changing trend was also observed in six provinces of Chongqing, Hebei, Inner Mongolia, Shanxi, Shaanxi, and Qinghai, but the urban area expected to expand within UGBs in these provinces was relatively lower. That is because SSP4 is a highly unequal development pathway within countries, under which the well-developed provinces will develop at a higher growth rate while the less developed provinces will grow following a constant progression rate (Chen et al., 2022). The first five provinces were located in eastern China with a relatively higher economic development level. Though these five provinces demonstrated with lower fertility rate under SSP4, they can still attract the migration of population from the provinces with lower socioeconomic development levels through the capitals to achieve population growth (Jiang et al., 2017). In addition to the provinces above, Sichuan also shows a similar tendency in urban land demand but has a relatively larger urban area expected to expand within UGBs under each scenario. This can be explained by the fact that, despite being located in the inland of western China, Sichuan has a relatively strong population base, and the urban expands rapidly with the population growth at the same time. In particular, the decrease in urban land demand under SSP1 and SSP5 was similar and was larger than those under other scenarios in Gansu, which can be related to the extremely low interprovincial floating population in this province (Liu et al., 2015).

4.3. Policy Suggestions

China should take measures to address the pressure of urban shrinkage. The simulation results under five SSPs indicate that most provinces in China will face urban shrinkage pressure, which will be much higher in the provinces of Heilongjiang, Jilin, and Liaoning (Figure 5). Measures to address urban shrinkage pressure can be classified into mitigation and adaptation (Sousa & Pinho, 2015). Measures of mitigation emphasize restoring urban vitality, revitalizing the urban economy, and promoting the urban population (Yang et al., 2017), market (Hu et al., 2021), capital (Rocak et al., 2016), and other reflowing factors to realize the regrowth of shrinking cities (Sousa & Pinho, 2015) when dealing with urban shrinkage. Measures of adaptation do not sidestep the problems posed by urban shrinkage but regard urban shrinkage as a development pattern equivalent to urban growth, trying to utilize and optimize the impacts of urban shrinkage. Measures with adaptive characteristics, including deconstructing (Bontje, 2004), revaluating (Nunes, 2008), reorganizing (Safransky, 2014), and imagining (Long & Wu, 2016), are taken to cope with urban vacant space, adjust urban morphology, and remodel urban space to promote urban development toward environmental conservation, harmony and diversification (Haase, Haase, Rink, et al., 2014; Thomas Elmqvist, 2013). China has currently adjusted family planning policies to alleviate urban shrinkage pressure (Yang & Dunford, 2018) and has proposed a control and reduction strategy for the total amount of construction land (Wang et al., 2021), elevating management on construction land reduction to a national development agenda (The State Council of PRC, 2015). In the future, measures of adaptation, including transforming inefficient vacant land to urban green space (Haase, Haase, Rink, et al., 2014; Wu & Li, 2019; Zhang et al., 2017), need to be taken into account to implement urban renewal action, further improve urban spatial structure and urban functional arrangements and transform the way of urban development and economic growth (The People's Government of Beijing Municipality, 2021) to mitigate the negative impacts of urban shrinkage.

The place-based urban expansion mode needs to be chosen in each province to promote urban sustainability. The evaluation results reveal that the negative impacts of urban expansion on ecosystem services are significantly

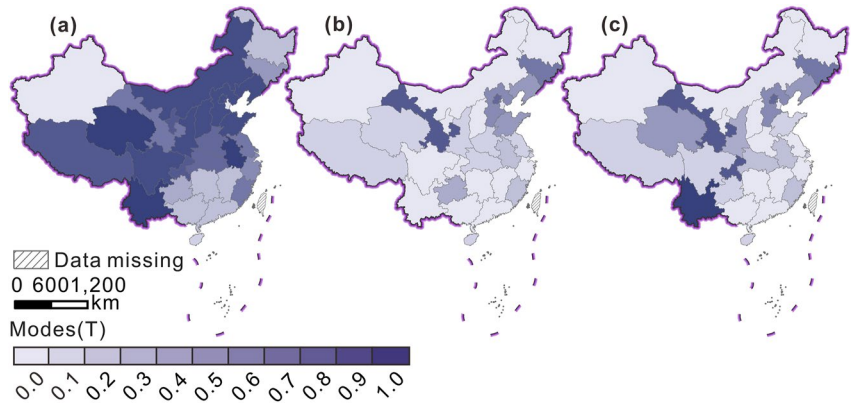

Figure 10. Urban expansion mode corresponding to minimum ecosystem service loss under shared socioeconomic pathway 1 (SSP1). *Note.* (a) To the loss of habitat quality. (b) To the loss of food production. (c) To the loss of carbon sequestration.

different under the 11 modes (Figure 10). Taking the SSP1 scenario as an example, in 14 provinces, including Beijing, Tianjin, Jilin, Heilongjiang, Shanghai, Jiangxi, Hunan, Guizhou, Guangdong, Guangxi, Hainan, Jiangsu, Gansu, and Xinjiang, urban expansion modes dominated by organic growth will result in lower ecosystem service losses than those dominated by spontaneous growth. A possible explanation might be that more high-quality cropland was projected to be invaded as the urban expansion mode shifts from organic growth to spontaneous growth. The proportion of bare land, rural residential land, and other construction land with lower NPP was projected to show a downward trend, which indicates that more land use/cover types with higher NPP will be occupied, leading to more carbon sequestration losses (Li et al., 2018), while the urban expansion modes dominated by spontaneous growth will result in the dispersion of urban patches, the reduction of patch aggregation and the fragmentation of habitats (Bao et al., 2015), leading to more severe losses of supporting services (Wu & Li, 2003; Yang & He, 2006). Thriteen provinces, including Hebei, Henan, Liaoning, Shandong, Zhejiang, Anhui, Hubei, Sichuan, Fujian, Inner Mongolia, Shanxi, Shaanxi, and Ningxia, will experience fewer losses of food production and carbon sequestration under the urban expansion modes dominated by organic growth and experience fewer losses of habitat quality under the urban expansion modes dominated by spontaneous growth. The main reason was that the cropland proportion of newly developed urban land was projected to exhibit an upward trend, while the proportions of forest, grassland, and other land use/cover types with high habitat suitability were projected to show a downward trend as the urban expansion mode shifts from organic growth to spontaneous growth. For Yunnan and Chongqing, the losses of food production will increase, and the losses of habitat quality and carbon sequestration will be alleviated as the urban expansion mode shifts from organic growth to spontaneous growth. The rise in the proportion of cropland and the decline in the proportion of forest will be the main reasons. Except for the losses of ecosystem services, the impacts of urban expansion modes on urban transportation, energy consumption, and infrastructure construction differ under diverse urban expansion modes as well (Hortas-Rico & Solé-Ollé, 2010; Johnson et al., 2021). Therefore, the optimal urban expansion mode needs to be determined in different provinces based on the type of ecosystem service preferentially protected and the differences in the environmental, social and economic impacts under diverse urban expansion modes to improve urban sustainability.

4.4. Future Perspectives

Future urban spatial patterns in China were simulated based on the localized SSPs and patch-based LUSD-urban model, and the UGBs of China in each province were delimited. Based on the delimitation results, the pressure of urban shrinkage from urban population decline and the possible impacts of future urban expansion on habitat quality, food production, and carbon sequestration were evaluated, providing scientific evidence for exploring China's urban development pathways.

Some limitation still needs to be noted. First, this study delimits UGBs based on the process of urban expansion. Limited by data availability, only the avoidance of high-quality cropland and nature reserves was taken into consideration, without fully considering the constraints of farmland redlines and ecological redlines on urban expansion (Jia et al., 2018). Second, in terms of ULD estimation, the urban population was used in this study

to estimate ULD according to the *National New Urbanization Planning (2014–2020)* (The State Council of PRC, 2014) without taking the impacts of economic growth on ULD into account. However, under the requirement of high-quality development, ULD will decrease as well after the GDP growth rate stabilizes, consistent with the estimated trend based on the urban population (Chen, Li, et al., 2020). Then, the seventh national population census data (National Bureau of Statistics of PRC, 2021) and the third-child policy (The State Council of PRC, 2021b) have not been considered in existing localized SSPs, leading to uncertainty in future ULD estimation. Third, in terms of urban spatial pattern simulation, the urban expansion was simulated at a 1-km resolution, which was lower than that in other studies at the scale of city or urban agglomeration. However, in view of this nationwide delineation on UGB, this study was not set to depict the UGBs in detail, but to delineate the future urban boundary roughly under diverse scenarios and urban expansion modes, so as to provide references for future urban spatial planning. At the same time, although this patch-based urban model mainly used at a relatively high spatial resolution, it can also simulate the differences in the spatial pattern of urban growth under diverse expansion modes with a spatial resolution of 1 km (Chen, Li, et al., 2020). In addition, this study does not fully consider the impacts of future transit construction (e.g., high-speed railways) (Zheng et al., 2012) and the development of urban agglomerations (Long et al., 2012) on future urban spatial patterns. Fourth, other driving factors other than population decline, such as economic depression, were not considered in the estimation of urban shrinkage pressure. In addition, limited by the large uncertainty on the spatial patterns of urban shrinkage, the urban shrinkage pressure was failed to be simulated spatially, but was only quantitatively estimated under diverse scenarios and expansion modes for each province.

In future work, under the premise of publicly released relevant data, we intend to first simulate urban expansion based on farmland redlines and ecological redlines to implement the strictest farmland protection system in UGB delimitation, ensure the total area of China's cropland to enhance food security (The State Council of PRC, 2021a) and optimize UGB delimitation combined with existing planning (Ministry of Natural Resources of PRC, 2020). In terms of ULD estimation, according to the seventh national population census data and the third-child policy, we will reestimate the future urban population and modify future ULD to more accurately simulate urban expansion. In terms of urban spatial pattern simulation, we will consider coupling patch-based urban model and hierarchical modeling strategy to delineate UGBs at a higher spatial resolution (Sun et al., 2020; Wang et al., 2022). Furthermore, we will fully consider the impacts of transportation and urban agglomeration development on the urban spatial pattern to optimize the urban expansion model and improve the reliability of the UGB. Last, we will consider taking other driving factors, such as GDP, into account to more accurately estimate urban shrinkage pressure. Furthermore, we will consider simulating urban shrinkage spatially to quantify China's spatial pattern of urban shrinkage pressure in the future.

5. Conclusions

This study simulated China's future urban dynamics and delimited China's UGBs at the provincial level under five SSPs and 11 modes. Based on the UGB delimitation results, provincial urban shrinkage pressure, occupancy on other land use/cover types and losses of ecosystem services were calculated, providing scientific evidence for urban planning in China.

China's ULD from 2021 to 2100 was projected to show an increasing trend followed by a decrease under the five SSPs. The extent of the UGB was projected to be 121,199–142,982 km^2, an increase of 34.14–58.25% compared with the ULA in 2020. The ULD of China in 2100 was projected to be 20.83–53.41% lower than the extent of UGBs, facing significant urban shrinkage pressure. Significant differences can be found in the occupancy on other land use/cover types of urban expansion and the losses of ecosystem services under diverse urban expansion modes. The changing trend of ULD, the pressure of urban shrinkage, the occupancy on other land use/cover types and the losses of ecosystem services all differ in different provinces.

Therefore, China, especially the three provinces of Heilongjiang, Jilin and Liaoning, should take measures of mitigation and adaptation to optimize urban spatial patterns and address urban shrinkage pressure. Optimal urban expansion modes need to be determined in different provinces based on the type of ecosystem service preferentially protected and the environmental, social, and economic characteristics to improve urban sustainability.

Data Availability Statement

All the data created in this study are openly available and the download information of supplementary data can be found in GitHub repositories with the identifier https://github.com/zfliu-bnu/Urban-growth-boundaries-of-China. The urban land data are collected from He et al. (2019). The land use/land cover data and the nature reserves data are available at http://www.resdc.cn. The DEM data are available at http://www.gscloud.cn. The NPP data are collected from He, Liu, et al. (2017). The GIS auxiliary data of administrative boundaries, city centers, roads and rivers are available at http://www.ngcc.cn. The provincial urban population census data of China are available at https://data.stats.gov.cn/. The provincial population and urban share data of China under localized SSPs are collected from Chen, Guo, et al. (2020).

Acknowledgments
This work was supported by the National Key R&D Program of China (Grant No. 2019YFA0607203) and the National Natural Science Foundation of China (41871185 and 41971271). It was also supported by the project from the State Key Laboratory of Earth Surface Processes and Resource Ecology, China.

References

Bao, Y., Liu, K., Li, T., & Hu, S. (2015). Effects of land use change on habitat based on InVEST model-taking Yellow river wetland nature reserve in Shaanxi province as an example (in Chinese). *Arid Zone Research*, *32*(3), 622–629. https://doi.org/10.13866/j.azr.2015.03.29

Bengston, D., & Yeo-Chang, Y. (2006). Urban containment policies and the protection of natural areas: The case of Seoul's Greenbelt. *Ecology and Society*, *11*(1), 3. https://doi.org/10.5751/ES-01504-110103

Bhatta, B. (2009). Modelling of urban growth boundary using geoinformatics. *International Journal of Digital Earth*, *2*(4), 359–381. https://doi.org/10.1080/17538940902971383

Bontje, M. (2004). Facing the challenge of shrinking cities in East Germany: The case of Leipzig. *Geojournal*, *61*(1), 13–21. doi https://doi.org/10.1007/s10708-005-0843-2

Cerreta, M., & De Toro, P. (2012). Urbanization suitability maps: A dynamic spatial decision support system for sustainable land use. *Earth System Dynamics*, *3*(2), 157–171. https://doi.org/10.5194/esd-3-157-2012

Chen, G., Li, X., Liu, X., Chen, Y., Liang, X., Leng, J., et al. (2020). Global projections of future urban land expansion under shared socioeconomic pathways. *Nature Communications*, *11*(1), 537. https://doi.org/10.1038/s41467-020-14386-x

Chen, J., Liu, Y., Zhang, E., Pan, T., & Liu, Y. (2022). Estimating China'S population over 21St century: Spatially explicit scenarios consistent with the shared socioeconomic pathways (SSPs). *Sustainability*, *14*(4), 2442. https://doi.org/10.3390/su14042442

Chen, Y. (2022). An Extended patch-based cellular automaton to simulate Horizontal and vertical urban growth under the shared socioeconomic pathways. *Computers, Environment and Urban Systems*, *91*, 101727. https://doi.org/10.1016/j.compenvurbsys.2021.101727

Chen, Y., Guo, F., Wang, J., Cai, W., Wang, C., & Wang, K. (2020). Provincial and gridded population projection for China under shared socioeconomic pathways from 2010 to 2100. *Scientific Data*, *7*(1), 83. https://doi.org/10.1038/s41597-020-0421-y

Chen, Y., Li, X., Liu, X., & Ai, B. (2014). Modeling urban land-use dynamics in a fast developing city using the modified logistic cellular automaton with a patch-based simulation strategy. *International Journal of Geographical Information Science*, *28*(2), 234–255. https://doi.org/10.1080/13658816.2013.831868

Chen, Y., Li, X., Liu, X., Huang, H., & Ma, S. (2019). Simulating urban growth boundaries using a patch-based cellular automaton with economic & ecological constraints. *International Journal of Geographical Information Science*, *33*(1), 55–80. https://doi.org/10.1080/13658816.2018.1514119

Chettry, V., & Surawar, M. (2021). Delineating urban growth boundary using remote sensing, ANN-MLP and CA model: A case study of Thiruvananthapuram urban agglomeration, India. *Journal of the Indian Society of Remote Sensing*, *49*(10), 2437–2450. https://doi.org/10.1007/s12524-021-01401-x

Cong, D., Zhao, S., Yu, T., Chen, C., & Wang, X. (2018). Urban growth boundary delimitation method integrating comprehensive ecological security pattern and urban expansion simulation -A case study of planning areas in Tianshui city (2015-2030). *Journal of Natural Resources*, *33*(1), 14–26. https://doi.org/10.11849/zrzyxb.20161330

Daniels, T. (2001). Smart growth: A new American approach to regional planning. *Planning Practice and Research*, *16*(3–4), 271–279. https://doi.org/10.1080/02697450120107880

Dorning, M. A., Koch, J., Shoemaker, D. A., & Meentemeyer, R. K. (2015). Simulating urbanization scenarios reveals Tradeoffs between conservation planning Strategies. *Landscape and Urban Planning*, *136*, 28–39. https://doi.org/10.1016/j.landurbplan.2014.11.011

Feng, Y., Wang, J., Tong, X., Liu, Y., Lei, Z., Gao, C., et al. (2018). The effect of observation scale on urban growth simulation using particle swarm optimization-based CA models. *Sustainability*, *10*(11), 4002. https://doi.org/10.3390/su10114002

Feng, Y., Wang, J., Tong, X., Shafizadeh-Moghadam, H., Cai, Z., Chen, S., et al. (2019). Urban expansion simulation and scenario prediction using cellular automata: Comparison between individual and multiple influencing factors. *Environmental Monitoring and Assessment*, *191*(5), 291. https://doi.org/10.1007/s10661-019-7451-y

Fragkias, M., & Seto, K. C. (2009). Evolving rank-size distributions of intra-metropolitan urban clusters in South China. *Computers, Environment and Urban Systems*, *33*(3), 189–199. https://doi.org/10.1016/j.compenvurbsys.2008.08.005

Gantumur, B., Wu, F., Vandansambuu, B., Tsegmid, B., Dalaibaatar, E., & Zhao, Y. (2020). Spatiotemporal dynamics of urban expansion and its simulation using CA-ANN model in Ulaanbaatar, Mongolia. *Geocarto International*, *37*(2), 494–509. https://doi.org/10.1080/10106049.2020.1723714

Gao, J., & O'Neill, B. C. (2020). Mapping global urban land for the 21st century with data-driven simulations and Shared Socioeconomic Pathways. *Nature Communications*, *11*(1), 2302. https://doi.org/10.1038/s41467-020-15788-7

Gennaio, M., Hersperger, A. M., & Bürgi, M. (2009). Containing urban sprawl—Evaluating effectiveness of urban growth boundaries set by the Swiss land Use plan. *Land Use Policy*, *26*(2), 224–232. https://doi.org/10.1016/j.landusepol.2008.02.010

Goldewijk, K. K., Beusen, A., Doelman, J., & Stehfest, E. (2017). Anthropogenic land use estimates for the Holocene - HYDE 3.2. *Earth System Science Data*, *9*(2), 927–953. https://doi.org/10.5194/essd-9-927-2017

Grimm, N. B., Faeth, S. H., Golubiewski, N. E., Redman, C. L., Wu, J., Bai, X., et al. (2008). Global change and the ecology of cities. *Science*, *319*(5864), 756–760. https://doi.org/10.1126/science.1150195

Guo, R., & Huang, M. (2018). Scenario simulation of Harbin urban expansion and its spatial pattern evaluation with GIS/RS. *Earth Resources and Environmental Remote Sensing/GIS Applications IX*, 10790. https://doi.org/10.1117/12.2501996

Haase, A., Bernt, M., Grossmann, K., Mykhnenko, V., & Rink, D. (2016). Varieties of shrinkage in European cities. *European Urban and Regional Studies*, *23*(1), 86–102. https://doi.org/10.1177/0969776413481985

Haase, A., Rink, D., Grossmann, K., Bernt, M., & Mykhnenko, V. (2014). Conceptualizing urban shrinkage. *Environment and Planning A-Economy and Space*, *46*(7), 1519–1534. https://doi.org/10.1068/a46269

Haase, D., Haase, A., & Rink, D. (2014). Conceptualizing the nexus between urban shrinkage and ecosystem services. *Landscape and Urban Planning*, *132*, 159–169. https://doi.org/10.1016/j.landurbplan.2014.09.003

Han, H., Lai, S., Dang, A., Tan, Z., & Wu, C. (2009). Effectiveness of urban construction boundaries in Beijing: An assessment. *Journal of Zhejiang University—Science*, *10*(9), 1285–1295. https://doi.org/10.1631/jzus.A0920317

He, C., Li, J., Zhang, X., Liu, Z., & Zhang, D. (2017). Will rapid urban expansion in the drylands of northern China continue: A scenario analysis based on the land Use scenario dynamics-urban model and the shared socioeconomic pathways. *Journal of Cleaner Production*, *165*, 57–69. https://doi.org/10.1016/j.jclepro.2017.07.018

He, C., Liu, Z., Gou, S., Zhang, Q., Zhang, J., & Xu, L. (2019). Detecting global urban expansion over the last three decades using a fully convolutional network. *Environmental Research Letters*, *14*(3), 034008. https://doi.org/10.1088/1748-9326/aaf936

He, C., Liu, Z., Wu, J., Pan, X., Fang, Z., Li, J., et al. (2021). Future global urban water scarcity and potential solutions. *Nature Communications*, *12*(1), 4667. https://doi.org/10.1038/s41467-021-25026-3

He, C., Liu, Z., Xu, M., Ma, Q., & Dou, Y. (2017). Urban expansion brought stress to food security in China: Evidence from decreased cropland net primary productivity. *Science of the Total Environment*, *576*, 660–670. https://doi.org/10.1016/j.scitotenv.2016.10.107

He, C., Okada, N., Zhang, Q., Shi, P., & Li, J. (2008). Modelling dynamic urban expansion processes incorporating a potential model with cellular automata. *Landscape and Urban Planning*, *86*(1), 79–91. https://doi.org/10.1016/j.landurbplan.2007.12.010

He, C., Okada, N., Zhang, Q., Shi, P., & Zhang, J. (2006). Modeling urban expansion scenarios by coupling cellular automata model and system dynamic model in Beijing, China. *Applied Geography*, *26*(3–4), 323–345. https://doi.org/10.1016/j.apgeog.2006.09.006

He, C., Zhang, D., Huang, Q., & Zhao, Y. (2016). Assessing the potential impacts of urban expansion on regional carbon storage by linking the LUSD-urban and InVEST models. *Environmental Modelling & Software*, *75*(SI), 44–58. https://doi.org/10.1016/j.envsoft.2015.09.015

Hortas-Rico, M., & Solé-Ollé, A. (2010). Does urban sprawl increase the costs of providing local public services? Evidence from Spanish municipalities. *Urban Studies*, *47*(7), 1513–1540. https://doi.org/10.1177/0042098009353620

Hu, T., Yang, J., Li, X., & Gong, P. (2016). Mapping urban land Use by using Landsat images and open social data. *Remote Sensing*, *8*(2), 151. https://doi.org/10.3390/rs8020151

Hu, Y., Wang, Z., & Deng, T. (2021). Expansion in the shrinking cities: Does place-based policy help to curb urban shrinkage in China? *Cities*, *113*, 103188. https://doi.org/10.1016/j.cities.2021.103188

Huang, Q., Liu, Z., He, C., Gou, S., Bai, Y., Wang, Y., et al. (2020). The occupation of cropland by global urban expansion from 1992 to 2016 and its implications. *Environmental Research Letters*, *15*(8), 084037. https://doi.org/10.1088/1748-9326/ab858c

Jia, K., Zhang, C., Yang, Y., & You, Z. (2019). Delimitation of urban growth boundary based on the coordination of ecology and residential activity spaces: A case study of Jinan, China. *Journal of Resources and Ecology*, *10*(5), 518–524. https://doi.org/10.5814/j.issn.1674-764X.2019.05.007

Jia, Z., Ma, B., Zhang, J., & Zeng, W. (2018). Simulating spatial-temporal changes of land-use based on ecological redline restrictions and landscape driving factors: A case study in Beijing. *Sustainability*, *10*(4), 1299. https://doi.org/10.3390/su10041299

Jiang, L., & O Neill, B. C. (2017). Global urbanization projections for the shared socioeconomic pathways. *Global Environmental Change*, *42*, 193–199. https://doi.org/10.1016/j.gloenvcha.2015.03.008

Jiang, P., Cheng, Q., Gong, Y., Wang, L., Zhang, Y., Cheng, L., et al. (2016). Using urban development boundaries to constrain uncontrolled urban sprawl in China. *Annals of the American Association of Geographers*, *106*(6), 1321–1343. https://doi.org/10.1080/24694452.2016.1198213

Jiang, T., Zhao, J., Cao, L., Wang, Y., Su, B., Jing, C., et al. (2018). Projection of national and provincial economy under the shared socioeconomic pathways in China (in Chinese). *Progressus Inquisitiones De Mutatione Climatis*, *14*(1), 50–58. https://doi.org/10.12006/j.issn.1673-1719.2017.161

Jiang, T., Zhao, J., Jing, C., Cao, L., Wang, Y., Sun, H., et al. (2017). National and provincial population projected to 2100 under the shared socioeconomic pathways in China (in Chinese). *Progressus Inquisitiones De Mutatione Climatis*, *13*(2), 128–137. https://doi.org/10.12006/j.issn.1673-1719.2016.249

Jiang, W., Chen, Z., Lei, X., He, B., Jia, K., & Zhang, Y. (2016). Simulation of urban agglomeration ecosystem spatial distributions under different scenarios: A case study of the Changsha-Zhuzhou-Xiangtan urban agglomeration. *Ecological Engineering*, *88*, 112–121. https://doi.org/10.1016/j.ecoleng.2015.12.014

Johnson, J. A., Kennedy, C. M., Oakleaf, J. R., Baruch-Mordo, S., Polasky, S., & Kiesecker, J. (2021). Energy matters: Mitigating the impacts of future land expansion will require managing energy and extractive footprints. *Ecological Economics*, *187*, 107106. https://doi.org/10.1016/j.ecolecon.2021.107106

Jun, M. (2004). The effects of Portland's urban growth boundary on urban development patterns and commuting. *Urban Studies*, *41*(7), 1333–1348. https://doi.org/10.1080/0042098042000214824

Kroll, F., & Kabisch, N. (2012). The relation of diverging urban growth processes and demographic change along an urban-rural gradient. *Population, Space and Place*, *18*(3), 260–276. https://doi.org/10.1002/psp.653

Li, J., Wang, Z., Lai, C., Wu, X., Zeng, Z., Chen, X., et al. (2018). Response of net primary production to land use and land cover change in mainland China since the late 1980s. *Science of the Total Environment*, *639*, 237–247. https://doi.org/10.1016/j.scitotenv.2018.05.155

Li, X., & Gong, P. (2016). Urban growth models: Progress and perspective. *Science Bulletin*, *61*(21), 1637–1650. https://doi.org/10.1007/s11434-016-1111-1

Li, X., Gong, P., Yu, L., & Hu, T. (2017). A segment derived patch-based logistic cellular automata for urban growth modeling with heuristic rules. *Computers, Environment and Urban Systems*, *65*, 140–149. https://doi.org/10.1016/j.compenvurbsys.2017.06.001

Li, X., Gong, P., Zhou, Y., Wang, J., Bai, Y., Chen, B., & Zhu, Z. (2020). Mapping global urban boundaries from the global artificial Impervious area (GAIA) data. *Environmental Research Letters*, *15*(9), 94044. https://doi.org/10.1088/1748-9326/ab9be3

Liang, X., Guan, Q., Clarke, K. C., Liu, S., Wang, B., & Yao, Y. (2021). Understanding the Drivers of sustainable land expansion using a patch-Generating land Use simulation (PLUS) model: A case study in Wuhan, China. *Computers, Environment and Urban Systems*, *85*, 101569. https://doi.org/10.1016/j.compenvurbsys.2020.101569

Liang, X., Liu, X., Li, X., Chen, Y., Tian, H., & Yao, Y. (2018). Delineating multi-scenario urban growth boundaries with a CA-based FLUS model and morphological method. *Landscape and Urban Planning*, *177*, 47–63. https://doi.org/10.1016/j.landurbplan.2018.04.016

Liu, H., Zhang, Z., Shui, W., Wang, Q., & Yang, Y. (2017). Urban growth boundary delimitation of resource-exhausted cities: A case study of Huaibei city (in Chinese). *Journal of Natural Resources*, *32*(3), 391–405. https://doi.org/10.11849/zrzyxb.20160425

Liu, T., Liu, M., Jing, L., & Li, T. (2021). An urban expansion simulation method of dual constrained RF-patch-CA considering the importance of driving factor (in Chinese). *Geography and Geo-Information Science*, *37*(2), 63–70. https://doi.org/10.3969/j.issn.1672-0504.2021.02.009

Liu, T., Qi, Y., & Cao, G. (2015). China's floating population in the 21st century: Uneven landscape, influencing factors, and effects on urbanization (in Chinese). *Acta Geographica Sinica*, *70*(4), 567–581. https://doi.org/10.11821/dlxb201504005

Liu, X., Lao, C., Li, X., Liu, Y., & Chen, Y. (2012). An integrated approach of remote sensing, GIS and swarm intelligence for zoning protected ecological areas. *Landscape Ecology*, *27*(3), 447–463. https://doi.org/10.1007/s10980-011-9684-1

Liu, X., Liang, X., Li, X., Xu, X., Ou, J., Chen, Y., & Pei, F. (2017). A future land use simulation model (FLUS) for simulating multiple land use scenarios by coupling human and natural effects. *Landscape and Urban Planning*, *168*, 94–116. https://doi.org/10.1016/j.landurbplan.2017.09.019

Liu, Z., He, C., Zhou, Y., & Wu, J. (2014). How much of the world's land has been urbanized, really? A hierarchical framework for avoiding confusion. *Landscape Ecology*, *29*(5), 763–771. https://doi.org/10.1007/s10980-014-0034-y

Long, Y., Gu, Y., & Han, H. (2012). Spatiotemporal heterogeneity of urban planning implementation effectiveness: Evidence from five urban master plans of Beijing. *Landscape and Urban Planning*, *108*(2–4), 103–111. https://doi.org/10.1016/j.landurbplan.2012.08.005

Long, Y., Han, H., Lai, S., & Mao, Q. (2013). Urban growth boundaries of the Beijing metropolitan area: Comparison of simulation and artwork. *Cities*, *31*, 337–348. https://doi.org/10.1016/j.cities.2012.10.013

Long, Y., Han, H., & Mao, Q. (2009). Establishing urban growth boundaries using constrained CA (in Chinese). *Acta Geographica Sinica*, *64*(8), 999–1008. https://doi.org/10.3321/j.issn:0375-5444.2009.08.010

Long, Y., & Mao, Q. (2010). A constrained CA model for planning simulation incorporating Institutional constraints. *City Planning Review*, *19*(1), 17–25.

Long, Y., & Wu, K. (2016). Several emerging issues of China's urbanization: Spatial expansion, population shrinkage, low-density human Activities and city boundary delimitation (in Chinese). *Urban Planning Forum*, *2*, 72–77. https://doi.org/10.16361/j.upf.201602009

Ma, S., Li, X., & Cai, Y. (2017). Delimiting the urban growth boundaries with a modified ant colony optimization model. Computers. *Environment and Urban Systems*, *62*, 146–155. https://doi.org/10.1016/j.compenvurbsys.2016.11.004

Meentemeyer, R. K., Tang, W., Dorning, M. A., Vogler, J. B., Cunniffe, N. J., & Shoemaker, D. A. (2013). Futures: Multilevel simulations of Emerging urban-rural landscape structure using a stochastic patch-growing algorithm. *Annals of the Association of American Geographers*, *103*(4), 785–807. https://doi.org/10.1080/00045608.2012.707591

Meng, S., Huang, Q., He, C., & Yang, S. (2018). Mapping the changes in supply and demand of carbon sequestration service: A case study in Beijing (in Chinese). *Journal of Natural Resources*, *33*(7), 1191–1203. https://doi.org/10.31497/zrzyxb.20171155

Millennium Ecosystem Assessment. (2005). *Ecosystems and human well-being: Synthesis*. Island Press.

Ministry of Housing and Urban-Rural Development of PRC. (2005). *Measures for formulating city planning (in Chinese)*. Ministry of Housing and Urban-Rural Development of PRC. Retrieved from http://www.gov.cn/ziliao/flfg/2006-02/15/content_191969.htm

Ministry of Land and Resources of PRC. (2009). *Guiding opinions on the overall planning for land use at the city, county and township levels (in Chinese)*. Ministry of Land and Resources of PRC. Retrieved from http://www.gov.cn/gzdt/2009-06/04/content_1331784.htm

Ministry of Natural Resources of PRC. (2020). *Guidelines for municipal territorial spatial master plan (in Chinese)*. Ministry of Natural Resources of PRC. Retrieved from http://www.gov.cn/xinwen/2020-09/25/content_5547144.htm

Mubarak, F. A. (2004). Urban growth boundary policy and residential suburbanization: Riyadh, Saudi Arabia. *Habitat International*, *28*(4), 567–591. https://doi.org/10.1016/j.habitatint.2003.10.010

Narayanan, A. (2006). Fast binary dilation/erosion algorithm using kernel subdivision. In P. J. Narayanan, S. K. Nayar, H. Y. Shum, P. J. Narayanan, S. K. Nayar, H. Y. Shum, et al. (Eds.), *Lecture Notes in Computer Science* (pp. 335–342). Springer.

National Bureau of Statistics of PRC. (2021). *The seventh national census communique (No. 7)-urban and rural population and floating population*(in Chinese). National Bureau of Statistics of PRC. Retrieved from http://www.gov.cn/xinwen/2021-05/11/content_5605791.htm

Ning, J., Liu, J., Kuang, W., Xu, X., Zhang, S., Yan, C., et al. (2018). Spatiotemporal patterns and characteristics of land-use change in China during 2010–2015. *Journal of Geographical Sciences*, *28*(5), 547–562. https://doi.org/10.1007/s11442-018-1490-0

Nunes, R. (2008). Book review: Shrinking cities: Volume 1: International research: Philipp Oswalt, 2005 Ostfildern-Ruit Hatje Cantz Verlag 735. €39.80 paperback ISBN 3 7757 1682 3 paperback. *Urban Studies*, *45*(5–6), 1301–1303. https://doi.org/10.1177/00420980080450051206

O'Neill, B. C., Kriegler, E., Ebi, K. L., Kemp-Benedict, E., Riahi, K., Rothman, D. S., et al. (2017). The roads ahead: Narratives for shared socioeconomic pathways describing world futures in the 21st century. *Global Environmental Change-Human and Policy Dimensions*, *42*, 169–180. https://doi.org/10.1016/j.gloenvcha.2015.01.004

O'Neill, B. C., Kriegler, E., Riahi, K., Ebi, K. L., Hallegatte, S., Carter, T. R., et al. (2014). A new scenario framework for climate change research: The concept of shared socioeconomic pathways. *Climatic Change*, *122*(3), 387–400. https://doi.org/10.1007/s10584-013-0905-2

Rocak, M., Hospers, G., & Reverda, N. (2016). Searching for social sustainability: The case of the shrinking city of Heerlen, The Netherlands. *Sustainability*, *8*(4), 382. https://doi.org/10.3390/su8040382

Safransky, S. (2014). Greening the urban Frontier: Race, property, and resettlement in Detroit. *Geoforum*, *56*, 237–248. https://doi.org/10.1016/j.geoforum.2014.06.003

Sakieh, Y., Amiri, B. J., Danekar, A., Feghhi, J., & Dezhkam, S. (2015). Simulating urban expansion and scenario prediction using a cellular automata urban growth model, SLEUTH, through a case study of Karaj City, Iran. *Journal of Housing and the Built Environment*, *30*(4), 591–611. https://doi.org/10.1007/s10901-014-9432-3

Seto, K. C., Guneralp, B., & Hutyra, L. R. (2012). Global forecasts of urban expansion to 2030 and direct impacts on biodiversity and carbon pools. *Proceedings of the National Academy of Sciences of the United States of America*, *109*(40), 16083–16088. https://doi.org/10.1073/pnas.1211658109

Sharp, R., Chaplin-Kramer, R., Wood, S., Guerry, A., Tallis, H., & Ricketts, T. (2016). *InVEST user 's guide, the natural capital project*. Stanford University, University of Minnesota, The Nature Conservancy, and World Wildlife Fund. https://doi.org/10.13140/RG.2.2.32693.78567

Soares-Filho, B. S., Coutinho Cerqueira, G., & Lopes Pennachin, C. (2002). Dinamica—A stochastic cellular automata model designed to simulate the landscape dynamics in an Amazonian colonization frontier. *Ecological Modelling*, *154*(3), 217–235. https://doi.org/10.1016/S0304-3800(02)00059-5

Song, S., Liu, Z., He, C., & Lu, W. (2020). Evaluating the effects of urban expansion on natural habitat quality by coupling localized shared socioeconomic pathways and the land use scenario dynamics-urban model. *Ecological Indicators*, *112*, 106071. https://doi.org/10.1016/j.ecolind.2020.106071

Sousa, S., & Pinho, P. (2015). Planning for shrinkage: Paradox or paradigm. *European Planning Studies*, *23*(1), 12–32. https://doi.org/10.1080/09654313.2013.820082

Sun, P., & Wang, K. (2021). Identification and stage division of urban shrinkage in the three provinces of northeast China. *Acta Geographica Sinica*, *76*(6), 1366–1379.

Sun, Y., Yang, J., Song, S., Zhu, J., & Dai, J. (2020). Modeling of multilevel vector cellular automata and its simulation of land use change(in Chinese). *Acta Geographica Sinica*, *75*(10), 2164–2179. https://doi.org/10.11821/dlxb202010009

Sun, Z., Liu, Z., He, C., & Wu, J. (2017). Impacts of urban expansion on ecosystem services in the drylands of northern China: A case study in the Hohhot-Baotou-Ordos urban agglomeration region (in Chinese). *Journal of Natural Resources*, *32*(10), 1691–1704. https://doi.org/10.11849/zrzyxb.20160928

Tan, R., Liu, Y., Liu, Y., & He, Q. (2020). A literature review of urban growth boundary: Theory, modeling, and effectiveness evaluation (in Chinese). *Progress in Geography*, *39*(2), 327–338. https://doi.org/10.18306/dlkxjz.2020.02.013

Tariq, A., & Shu, H. (2020). CA-Markov chain analysis of seasonal land surface temperature and land use land cover change using optical multi-temporal satellite data of Faisalabad, Pakistan. *Remote Sensing*, *12*(20), 3402. https://doi.org/10.3390/rs12203402

Tayyebi, A., Pijanowski, B. C., & Tayyebi, A. H. (2011). An urban growth boundary model using neural networks, GIS and radial parameterization: An application to Tehran, Iran. *Landscape and Urban Planning*, *100*(1–2), 35–44. https://doi.org/10.1016/j.apgeog.2011.01.018

The Nature of 2040. (2000). The nature of 2040: The Region's 50-year plan for managing growth. Retrieved from https://pdxscholar.library.pdx.edu/oscdl_metro/34/

The People's Government of Beijing Municipality. (2021). Urban regeneration action plan of Beijing (in Chinese) (pp. 2021–2025). Retrieved from http://www.beijing.gov.cn/zhengce/zhengcefagui/202108/t20210831_2480185.html

The State Council of PRC. (2011). *Regulation on the protection of basic farmlands (in Chinese)*. The State Council of PRC. Retrieved from http://www.gov.cn/gongbao/content/2011/content_1860862.htm

The State Council of PRC. (2014). *National new urbanization planning (2014–2020) (in Chinese)*. The State Council of PRC. Retrieved from http://www.gov.cn/gongbao/content/2014/content_2644805.htm

The State Council of PRC. (2015). *Integrated reform plan for promoting ecological progress (in Chinese)*. The State Council of PRC. Retrieved from http://www.gov.cn/guowuyuan/2015-09/21/content_2936327.htm

The State Council of PRC. (2021a). *Regulation on the Implementation of the land administration law of the People's Republic of China*(in Chinese). The State Council of PRC. Retrieved from http://www.gov.cn/zhengce/content/2021-07/30/content_5628461.htm

The State Council of PRC. (2021b). *Third-child policy to unleash childbirth potential*(in Chinese). The State Council of PRC. Retrieved from http://www.gov.cn/zhengce/2021-07/20/content_5626190.htm

Thomas Elmqvist, M. F. J. G. (2013). *Urbanization, biodiversity and ecosystem services: Challenges and opportunities*. Springer.

van Asselen, S., & Verburg, P. H. (2013). Land cover change or land-use intensification: Simulating land system change with a global-scale land change model. *Global Change Biology*, *19*(12), 3648–3667. https://doi.org/10.1111/gcb.12331

Wang, F., & Marceau, D. J. (2013). A patch-based cellular automaton for simulating land-use changes at fine spatial resolution. *Transactions in GIS*, *17*(6), 828–846. https://doi.org/10.1111/tgis.12009

Wang, H., Wu, Y., Deng, Y., & Xu, S. (2022). Model construction of urban agglomeration expansion simulation considering urban Flow and hierarchical characteristics. *Journal of Geographical Sciences*, *32*(3), 499–516. https://doi.org/10.1007/s11442-022-1958-9

Wang, J., Yang, Z., & Qian, X. (2020). Driving factors of urban shrinkage: Examining the role of local industrial diversity. *Cities*, *99*, 102646. https://doi.org/10.1016/j.cities.2020.102646

Wang, K., Li, G., & Liu, H. (2021). Porter effect test for construction land reduction. *Land Use Policy*, *103*, 105310. https://doi.org/10.1016/j.landusepol.2021.105310

Wang, Y., Gu, Z., & Li, X. (2014). Research progress of urban growth boundary at home and abroad(in Chinese). *Urban Planning International*, *29*(4), 1–11.

Wang, Y., Yin, X., & Li, G. (2012). Delimitation of urban growth boundary based on land ecological suitability evaluation: A case of Shenshan special corporation zone(in Chinese). *Urban Development Studies*, *19*(11), 76–82. https://doi.org/10.3969/j.issn.1006-3862.2012.11.012

Wei, Y. D., & Ye, X. (2014). Urbanization, urban land expansion and environmental change in China. *Stochastic Environmental Research and Risk Assessment*, *28*(4), 757–765. https://doi.org/10.1007/s00477-013-0840-9

Wu, J. (2013). Landscape sustainability science: Ecosystem services and human well-being in changing landscapes. *Landscape Ecology*, *28*(6), 999–1023. https://doi.org/10.1007/s10980-013-9894-9

Wu, J. (2014). Urban ecology and sustainability: The state-of-the-science and future directions. *Landscape and Urban Planning*, *125*(SI), 209–221. https://doi.org/10.1016/j.landurbplan.2014.01.018

Wu, J. (2021). Landscape sustainability science (II): Core questions and key approaches. *Landscape Ecology*, *36*(8SI), 2453–2485. https://doi.org/10.1007/s10980-021-01245-3

Wu, J., Mao, J., Lin, Q., & Li, J. (2017). Urban growth boundary based on the evaluation of habitat quality: Taking the Yangtze River Delta as an example (in Chinese). *Scientia Geographica Sinica*, *37*(1), 28–36. https://doi.org/10.13249/j.cnki.sgs.2017.01.004

Wu, K., & Li, Y. (2019). Research progress of urban land use and its ecosystem services in the context of urban shrinkage (in Chinese). *Journal of Natural Resources*, *34*(5), 1121–1134. https://doi.org/10.31497/zrzyxb.20190517

Wu, Z., & Li, Y. (2003). Effects of habitat fragmentation on survival of animal populations. *Acta Ecologica Sinica*, *23*(11), 2424–2435. (in Chinese). https://doi.org/10.3321/j.issn:1000-0933.2003.11.027

Xu, K., Wu, S., Chen, D., Dai, L., & Zhou, S. (2013). The urban growth boundary Determination based on Hydrology effect: Taking Xinminzhou as an example(in Chinese). *Scientia Geographica Sinica*, *33*(8), 979–985. https://doi.org/10.13249/j.cnki.sgs.2013.08.012

Yang, F., & He, D. (2006). Effects of habitat fragmentation on biodiversity(in Chinese). *Ecologic Science*, *25*(6), 564–567. https://doi.org/10.3969/j.issn.1008-8873.2006.06.020

Yang, J., Gong, J., Tang, W., Shen, Y., Liu, C., & Gao, J. (2019). Delineation of urban growth boundaries using a patch-based cellular automata model under multiple spatial and socio-economic scenarios. *Sustainability*, *11*(21), 6159. https://doi.org/10.3390/su11216159

Yang, Y., Wu, J., Wang, Y., Huang, Q., & He, C. (2021). Quantifying spatiotemporal patterns of shrinking cities in urbanizing China: A novel approach based on time-series nighttime light data. *Cities*, *118*, 103346. https://doi.org/10.1016/j.cities.2021.103346

Yang, Y., Zhang, L., Ye, Y., & Wang, Z. (2019). Curbing sprawl with development-limiting boundaries in urban China: A review of literature. *Journal of Planning Literature*, *35*(1), 25–40. https://doi.org/10.1177/0885412219874145

Yang, Z. (2019). Sustainability of urban development with population decline in different policy scenarios: A case study of northeast China. *Sustainability*, *11*(22), 6442. https://doi.org/10.3390/su11226442

Yang, Z., Cai, J., Qi, W., Liu, S., & Deng, Y. (2017). The influence of income, lifestyle, and green spaces on interregional migration: Policy implications for China. *Population, Space and Place*, *23*(2), e1996. https://doi.org/10.1002/psp.1996

Yang, Z., & Dunford, M. (2018). City shrinkage in China: Scalar processes of urban and hukou population losses. *Regional Studies*, *52*(8), 1111–1121. https://doi.org/10.1080/00343404.2017.1335865

Ye, S., Song, C., Shen, S., Gao, P., Cheng, C., Cheng, F., & Zhu, D. (2020). Spatial pattern of arable land-use intensity in China. *Land Use Policy*, *99*, 104845. https://doi.org/10.1016/j.landusepol.2020.104845

Ye, Y., Su, Y., Zhang, H., Liu, K., & Wu, Q. (2015). Construction of an ecological resistance surface model and its application in urban expansion simulations. *Journal of Geographical Sciences*, *25*(2). http://doi.org/10.1007/S11442-015-1163-1

Zhang, D., Liu, X., Lin, Z., Zhang, X., & Zhang, H. (2020). The delineation of urban growth boundaries in complex ecological environment areas by using cellular automata and a dual-environmental evaluation. *Journal of Cleaner Production*, *256*, 120361. https://doi.org/10.1016/j.jclepro.2020.120361

Zhang, J., Feng, C., & Chen, H. (2017). International research and China's exploration of urban shrinking(in Chinese). *Urban Planning International*, *32*(5), 1–9. https://doi.org/10.22217/upi.2016.551

Zhang, Q., Ban, Y., Liu, J., & Hu, Y. (2011). Simulation and analysis of urban growth scenarios for the Greater Shanghai Area, China. *Computers, Environment and Urban Systems*, *35*(2), 126–139. https://doi.org/10.1016/j.compenvurbsys.2010.12.002

Zheng, K., Xu, X., Zhang, X., & Liu, L. (2012). Spatial-temporal characteristics and future prediction of urban expansion in Shanghai (in Chinese). *Journal of Geo-Information Science*, *14*(4), 490–496. https://doi.org/10.3724/SP.J.1047.2012.00490

Zhou, Y., Varquez, A. C. G., & Kanda, M. (2019). High-resolution global urban growth projection based on multiple applications of the SLEUTH urban growth model. *Scientific Data*, *6*, 34. https://doi.org/10.1038/s41597-019-0048-z